The Development of Colitogenic CD4$^+$ T Cells Is Regulated by IL-7 in Collaboration with NK Cell Function in a Murine Model of Colitis

Osamu Yamaji,*,[1] Takashi Nagaishi,*,[1] Teruji Totsuka,* Michio Onizawa,* Masahiro Suzuki,* Naoto Tsuge,* Atsuhiko Hasegawa,† Ryuichi Okamoto,* Kiichiro Tsuchiya,* Tetsuya Nakamura,* Hisashi Arase,‡,§,¶ Takanori Kanai,‖ and Mamoru Watanabe*

We previously reported that IL-7$^{-/-}$RAG$^{-/-}$ mice receiving naive T cells failed to induce colitis. Such abrogation of colitis may be associated with not only incomplete T cell maintenance due to the lack of IL-7, but also with the induction of colitogenic CD4$^+$ T cell apoptosis at an early stage of colitis development. Moreover, NK cells may be associated with the suppression of pathogenic T cells in vivo, and they may induce apoptosis of CD4$^+$ T cells. To further investigate these roles of NK cells, RAG$^{-/-}$ and IL-7$^{-/-}$RAG$^{-/-}$ mice that had received naive T cells were depleted of NK cells using anti-asialo GM1 and anti-NK1.1 Abs. NK cell depletion at an early stage, but not at a later stage during colitogenic effector memory T cell (T_{EM}) development, resulted in exacerbated colitis in recipient mice even in the absence of IL-7. Increased CD44$^+$CD62L$^-$ T_{EM} and unique CD44$^-$CD62L$^-$ T cell subsets were observed in the T cell-reconstituted RAG$^{-/-}$ recipients when NK cells were depleted, although Fas, DR5, and IL-7R expressions in this subset differed from those in the CD44$^+$CD62L$^-$ T_{EM} subset. NK cell characteristics were the same in the presence or absence of IL-7 in vitro and in vivo. These results suggest that NK cells suppress colitis severity in T cell-reconstituted RAG$^{-/-}$ and IL-7$^{-/-}$RAG$^{-/-}$ recipient mice through targeting of colitogenic CD4$^+$CD44$^+$CD62L$^-$ T_{EM} and, possibly, of the newly observed CD4$^+$CD44$^-$CD62L$^-$ subset present at the early stage of T cell development. *The Journal of Immunology*, **2012, 188: 2524–2536.**

The pathogenesis of inflammatory bowel diseases (IBD), such as Crohn's disease and ulcerative colitis in humans, is known to be associated with dysregulated immune responses to luminal contents including Ags derived from commensal bacteria in gut. In patients with Crohn's disease, for example, excessive amounts of proinflammatory cytokines, such as IFN-γ, TNF, and IL-17 (1), are secreted predominantly by CD4$^+$ T cells infiltrating colonic tissues. The activities of these cells are thought to reflect the severity of IBD. Additionally, it is known that adoptive transfer of CD4$^+$ naive T cells into lymphopenic immune-deficient animals, such as SCID and RAG$^{-/-}$ mice, induces chronic inflammation in the colon and is considered an animal model of IBD (2, 3).

IL-7 is an important cytokine that is associated with the proliferation of immature B and T cells (4) as well as with homeostatic maintenance of peripheral T cells in vivo (5, 6). We have previously reported that IL-7 is secreted by intestinal epithelia, especially goblet cells (7), and that spontaneous colitis that is similar to IBD in humans is induced in transgenic mice overexpressing IL-7 (8). Additionally, we have shown that the IL-7R^{high}CD4$^+$ T cell subset is pathogenic (9) when the cells are transferred into RAG$^{-/-}$ mice (10, 11). Moreover, we have also shown that adoptive transfer of naive T cells in RAG and IL-7 double-deficient (IL-7$^{-/-}$RAG$^{-/-}$) mice fails to induce colitis (10). Therefore, IL-7 was initially considered to be essential for the induction of colitis. However, it is known that IL-7 is not required for the in vitro differentiation from naive T cells into Th1 or Th17 cells (12). It is also known that the spontaneous proliferation, which is dependent on Ag ligation to the CD3/TCR complex, can be observed even in the T cell-reconstituted IL-7$^{-/-}$RAG$^{-/-}$ re-

*Department of Gastroenterology and Hepatology, Graduate School of Medical Science, Tokyo Medical and Dental University, Tokyo 113-8519, Japan; †Department of Immunotherapeutics, Graduate School of Medical Science, Tokyo Medical and Dental University, Tokyo 113-8519, Japan; ‡Laboratory of Immunochemistry, World Premier International Research Center, Immunology Frontier Research Center, Osaka University, Osaka 565-0871, Japan; §Department of Immunochemistry, Research Institute for Microbial Diseases, Osaka University, Osaka 565-0871, Japan; ¶Japan Science and Technology, Core Research for Evolutional Science and Technology, Saitama 332-0012, Japan; and ‖Department of Gastroenterology, Keio University School of Medicine, Tokyo 160-8582, Japan

[1]O.Y. and T.N. contributed equally to this work.

Received for publication February 11, 2011. Accepted for publication January 10, 2012.

This work was supported in part by Grants-in-Aid for Scientific Research (to T. Nagaishi, T.T., R.O., K.T., T. Nakamura, T.K., and M.W.), for Scientific Research on Priority Areas (to M.W.), and for Exploratory Research and Creative Scientific Research (to M.W.) from the Japanese Ministry of Education, Culture, Sports, Science, and Technology; the Japanese Ministry of Health, Labor, and Welfare (to M.W.); the Japan Medical Association (to M.W.); the Terumo Life Science Foundation (to M.W.); the Ohyama Health Foundation (to M.W.); the Yakult Bio-Science Foundation (to T.K. and T.T.); the Research Fund of Mitsukoshi Health and Welfare Foundation (to M.W. and R.O.); the Japan Foundation for Applied Enzymology (to M.O.); the Japan Health Sciences Foundation (to M.O.); the Memorial Fund of Nihon University Medical Alumni Association (to T. Nagaishi); the Abbott Japan Allergy Research Award (to T. Nagaishi); the Foundation for Advancement of International Science (to T. Nagaishi); and the Takeda Science Foundation (to T. Nagaishi).

Address correspondence and reprint requests to Dr. Mamoru Watanabe and Dr. Takashi Nagaishi, Department of Gastroenterology and Hepatology, Graduate School of Medical Science, Tokyo Medical and Dental University, 1-5-45 Yushima, Bunkyo-ku, Tokyo 113-8519, Japan. E-mail addresses: mamoru.gast@tmd.ac.jp (M.W.) and tnagaishi.gast@tmd.ac.jp (T.N.)

The online version of this article contains supplemental material.

Abbreviations used in this article: ASGM1, asialo GM1; EAE, experimental autoimmune encephalomyelitis; IBD, inflammatory bowel disease; LP, lamina propria; LPL, lamina propria lymphocyte; PI, propidium iodide; SPL, spleen; T_{EM}, effector memory T cell; WT, wild-type.

www.jimmunol.org/cgi/doi/10.4049/jimmunol.1100371

cipient mice (13, 14). Additionally, our recent studies suggested that effector $CD4^+$ T cells were able to induce colitis even in IL-$7^{-/-}$RAG$^{-/-}$ mice that were parabiosed with colitic RAG$^{-/-}$ mice that had been injected with naive T cells 6 wk previously (15). Moreover, a deparabiosed IL-$7^{-/-}$RAG$^{-/-}$ mouse, which was surgically separated from T cell-receiving RAG$^{-/-}$–IL-$7^{-/-}$ RAG$^{-/-}$ parabionts 6 wk after the initial surgery, still maintained chronic colitis for at least another 12 wk (16). These results suggested that the abrogation of colitis in the T cell-reconstituted IL-$7^{-/-}$RAG$^{-/-}$ mice may be associated with not only incomplete T cell maintenance due to the lack of IL-7, but also with another mechanism by which the colitogenic $CD4^+$ T cell development is suppressed.

It is known that NK cells are responsible for innate immune responses, including the depletion of tumor cells or cells infected with various kinds of viruses (17). Additionally, NK cells induce inflammation in tissues by the production of proinflammatory cytokines such as IFN-γ (18, 19). In contrast, NK cells are also known to be critical for anti-inflammatory effects in the context of autoimmune diseases (20, 21). It has been reported that NK cells abrogate disease severity of experimental autoimmune encephalomyelitis (EAE) due to the suppression of pathogenic T cells (22, 23). It has also been reported that depletion of NK cells results in enhanced severity of a chronic colitis model (24). However, the mechanisms by which NK cells regulate inflammation in this colitis model have not been well described. In this regard, we hypothesized that the abrogation of colitogenic T cell development that we observed in naive T cell-receiving IL-$7^{-/-}$RAG$^{-/-}$ mice is associated with the effect of NK cells. We therefore focused our analysis of this phenomenon on NK cells.

Materials and Methods

Animals

Wild-type (WT) C57BL/6 mice were purchased from Japan CLEA (Tokyo, Japan). Rag-deficient (RAG$^{-/-}$) mice on a C57BL/6 background were obtained from Taconic (Hudson, NY) and the Central Laboratories for Experimental Animals (Kanagawa, Japan). IL-$7^{-/-}$ mice were provided by Dr. R. Zamoyska (National Institute for Medical Research, London, U.K.) and were intercrossed with RAG$^{-/-}$ to generate IL-$7^{-/-}$RAG$^{-/-}$ mice. Mice were maintained under specific pathogen-free conditions in the Animal Care Facility of Tokyo Medical and Dental University. Donors and recipients were used between 8 and 16 wk age. All animal experimentations were approved by the Animal Review Board of Tokyo Medical and Dental University and were performed in accordance with institutional guidelines.

Abs

The following mAbs and reagents were obtained from BD Pharmingen (San Jose, CA): anti-CD3ε (145-2C11), anti-CD4 (RM4-5), anti-CD11b (M1/70), anti-CD11c (HL3), anti-CD27 (LG.3A10), anti-CD28 (37.51), anti-CD43 (S7), anti-CD44 (IM7), anti-CD45RB (16A), anti-CD51 (RMV-7), anti-CD62L (MEL-14), anti-CD69 (H1.2F3), anti-CD94 (18d3), anti-CD95, anti-CD178 (MFL4), anti-CD244.2 (2B4 B6 alloantigen), anti-Ly49C,I (5E6), anti-Ly49D (4E5), anti-Ly49F (HBF-719), anti-Ly49G2 (4D11), anti–IL-7Rα (A7R34), anti-NK1.1 (PK136), and streptavidin. Biotin-conjugated anti-mouse NKG2A/C/E, biotin-conjugated anti-mouse IL-7Rα (A7R34), FITC-conjugated anti-mouse pan-NK cells (CD49b), and FITC-conjugated anti-mouse CD3ε (145-2C11) mAbs were purchased from eBioscience (San Diego, CA).

Flow cytometry (FACS)

To detect the cell surface expression of a variety of molecules, isolated mononuclear cells from individual organs including spleen (SPL), mesenteric lymph node (MLN), and colonic lamina propria (LP) were analyzed by FACS using standard staining methods. Briefly, the cells were suspended in PBS containing 2% FBS, which was used as the suspension fluid for subsequent staining, preincubated with an FcγR-blocking mAb (anti-CD16/32; 2.4G2; BD Biosciences) for 15 min to prevent nonspecific binding by the secondary Ab, and washed with suspension fluid followed by staining with specific FITC-, PE-, PerCP-, allophycocyanin-, or biotin-labeled Abs for 20 min on ice. Standard two-, three-, or four-color flow cytometric analyses were performed using the FACSCalibur (Becton Dickinson, Sunnyvale, CA) with appropriate software (CellQuest; BD Biosciences). Background fluorescence was also assessed by staining with control irrelevant isotype-matched mAbs.

NK cell depletion in vivo

The anti-asialo GM1 (ASGM1) polyclonal Ab was obtained from Wako Chemicals (Osaka, Japan) and reconstituted according to the manufacturer's specifications. The anti-NK1.1 mAb was affinity purified from the culture supernatant of a hybridoma clone, PK136, obtained from the American Type Culture Collection (Manassas, VA). For effective depletion of NK cells in vivo, either the anti-ASGM1 polyclonal Ab (0.25 mg/mouse) or anti-NK1.1 mAb (0.5 mg/mouse) was injected i.p. into mice (25) at the indicated time points in each experiment. The same amount of rabbit Ig (Rockland Immunochemicals, Gilbertsville, PA) or mouse IgG2a (Medical & Biological Laboratories, Nagoya, Japan) were used as the controls, respectively, for some of experiments. Effective (~95%) depletion of NK cells in vivo was confirmed by FACS analysis of single cells derived from individual organs such as SPL, MLN, and colonic LP.

Purification of naive T cell subsets and induction of colitis

For naive T cell purification, splenic mononuclear cells were obtained from WT mice and $CD4^+$ T cells were isolated using anti-CD4 (L3T4) MACS magnetic beads (Miltenyi Biotec, Bergisch Gladbach, Germany) according to the manufacturer's instructions. Enriched $CD4^+$ T cells (94–97% pure as estimated by FACS) were then labeled with PerCP- or allophycocyanin-conjugated anti-CD4, PE- or allophycocyanin-conjugated anti-CD44, and FITC-conjugated anti-CD62L. Subpopulations of $CD4^+$ cells were generated by three-color sorting on a FACSAria (Becton Dickinson). All populations were 98.0% pure on reanalysis. To induce an animal model of chronic colitis, 5×10^5 $CD4^+CD44^-CD62L^+$ (naive) T cells were adoptively transferred i.p. into 8- to 12-wk-old RAG$^{-/-}$ or IL-$7^{-/-}$RAG$^{-/-}$ recipient mice as previously described (2, 3, 10).

Isolation of LP lymphocytes

LP lymphocytes (LPL) were isolated from healthy or colitic mice as previously described (10). Briefly, RAG$^{-/-}$ or IL-$7^{-/-}$RAG$^{-/-}$ recipient mice were sacrificed 6–12 wk after injection of naive T cells to induce colitis. The entire length of the colon was removed, opened longitudinally, washed with PBS, and cut into small pieces. The dissected tissues were incubated with Ca^{2+}-, Mg^{2+}-free HBSS containing 1 mM DTT (Sigma-Aldrich, St. Louis, MO) for 45 min to remove mucus, and the epithelial layer was then treated with 3.0 mg/ml collagenase (Roche Diagnostics, Mannheim, Germany) and 0.01% DNase (Worthington Biomedical, Freehold, NJ) for 2 h. The cells were pelleted, washed twice with PBS, and were then subjected to density gradient centrifugation using 40–75% isotonic Percoll (Amersham Biotech, Piscataway, NJ) solution diluted with HBSS. Isolated whole LP mononuclear cells were subjected to FACS to analyze each lymphocyte subset. In some experiments, such LP mononuclear cells were further labeled with allophycocyanin-conjugated anti-CD4 and FITC-conjugated anti-CD3 to isolate colitogenic $CD4^+$ T cell subsets by FACSAria. All populations were 98.0% pure on reanalysis. Isolated LP $CD4^+$ T cells were subjected to cytokine production and cytotoxicity assays.

Determination of clinical score of colitis

The clinical score of colitis was determined using previously described methods (26) with minor modifications and was assessed by trained individuals blinded to the treatment group. Briefly, initial body weight and wasting, hunching over, piloerection, diarrhea, and blood in the stool or per rectum of the T cell-receiving RAG$^{-/-}$ or IL-$7^{-/-}$RAG$^{-/-}$ recipient mice were assessed when sacrificed. For wasting, weight loss of <20% from baseline was assigned 0 points and weight loss of >20% was assigned 1 point. For hunched over appearance, no obvious hunching was assigned 0 point, and extensive hunching was assigned as 1 point. For colon thickening, normal features were assigned 0 points, mild thickening was assigned 1 point, moderate thickening was assigned 2 points, and severe thickening was assigned 3 points. For stool consistency, 0 points were assigned to well-formed pellets, 1 point to pasty and semiformed stools that did not adhere to the anus, and 2 points to liquid stools that did adhere to the anus. An additional point was added if gross blood was noted. The scores of these parameters were added, resulting in a total clinical score ranging from 0 (healthy) to 8 (maximal colitis activity).

Histopathological examination of colitis

Mice receiving naive T cells were sacrificed 6 or 12 wk after the T cell transfer, and colonic specimens taken from proximal, middle, and distal colons were subjected to histopathological assessment. For this assessment, tissue samples were fixed in 10% neutral-buffered formalin. Paraffin-embedded sections (5 μm) were stained with H&E. The H&E-stained sections were analyzed without prior knowledge of the type of donors, recipients, and treatments. The degree of inflammation in the colon was graded according to a modification of the previously described scoring system (26, 27). Briefly, for mucosal damage, 0 points were assigned to normal appearance, 1 point to discrete lymphoepithelial lesions, 2 points to diffuse crypt elongation, and 3 points to extensive crypt elongation or mucosal erosion/ulceration. For cell infiltration the points assigned were: 0, to normal, or presence of occasional leukocytes; 1, to widely scattered leukocytes or focal aggregates of leukocytes; 2, to confluence of leukocytes extending into the submucosa with focal effacement of the muscularis; 3, to transmural extension of leukocyte infiltration. For crypt abscess, the assigned points were: 0, to no crypt abscess; 1, to the presence of crypt abscess. The cumulative degree of these parameters was calculated as a total histological score ranging from 0 (no change) to 21 (extensive cell infiltration and tissue damage).

ELISA

To measure cytokine production, 1×10^5 LP $CD4^+$ T cells were cultured in 200 μl RPMI 1640 (Sigma-Aldrich) supplemented with 10% heat-inactivated FBS, 500 U/ml penicillin, 100 μg/ml streptomycin (Sigma-Aldrich), 10 mM HEPES, 1% nonessential amino acids, and 50 μM 2-ME (Life Technologies Invitrogen, Carlsbad, CA), termed complete RPMI 1640, in the presence of 5 μg/ml plate-bound anti-CD3ε (145-2C11) and 2 μg/ml soluble anti-CD28 (37.51) mAbs on flat-bottom 96-well plates (Costar, Cambridge, MA) at 37°C in a humidified atmosphere incubator containing 5% CO_2 for 48 h. Culture supernatants were removed and analyzed for the production of cytokines such as IFN-γ, TNF, and IL-17. Cytokine concentrations were determined using specific ELISAs (R&D Systems, Minneapolis, MN) as per the manufacturer's recommendations.

Isolation of NK cells and cytotoxicity assay

Spleen cell suspensions were prepared from $RAG^{-/-}$ or IL-$7^{-/-}RAG^{-/-}$ mice and treated with NH_4Cl buffer to remove erythrocytes. The NK cell population was then labeled with FITC-conjugated anti-DX5 (CD49b) and isolated for use as effector cells in the cytotoxicity assay by sorting on a FACSAria. The purity of isolated NK cells was 98.0% on reanalysis. To measure cytokine production, 5×10^4 NK cells were cultured in 200 μl RPMI 1640 supplemented with 10% FBS, 500 U/ml penicillin, and 100 μg/ml streptomycin in the presence of 100 ng/ml rIL-2, 100 ng/ml rIL-12, and 100 ng/ml rIL-18 on flat-bottom 96-well plates at 37°C in a humidified atmosphere incubator containing 5% CO_2. Culture supernatants were removed after 24 h and analyzed for IFN-γ production. Cytotoxicity assays were performed using the flow cytometric method reported by Xu et al. (28; see also Ref. 29). Briefly, isolated naive T cells from WT mice or LP effector memory T cells (T_{EM}) from colitic mice were labeled with a lipophilic green fluorescent cell linker, PKH2 (Sigma-Aldrich), which is incorporated into the plasma membrane. Uniform labeling of cells was confirmed by flow cytometry. Labeled 5×10^4 target T cells were coincubated in round-bottom 96-well plates (Costar) with effector NK cells (T:E ratio, 1:5 to 1:0.6) in complete RPMI 1640 supplemented with 100 ng/ml rIL-2 (PeproTech, London, U.K.) with or without 50 ng/ml rIL-7 (PeproTech) at 37°C in humidified air containing 5% CO_2 for 4 h. Naive T cells or LP colitogenic T cells that were incubated under the same conditions but without effector NK cells were also prepared as controls. Cells were then collected, stained with propidium iodide (PI), and analyzed by FACS. Cytotoxic activity was determined by calculating the percentage of the double-positive population for both PI (FL2) and PKH2 (FL1). In some experiments, a mouse lymphoma cell line, YAC-1, obtained from the American Type Culture Collection, was used as target cells for a [^{51}Cr] release assay with the standard protocol. Briefly, target cells were labeled with 3.7 MBq of $Na_2[^{51}Cr]O_4$ for 1 h at 37°C and washed three times with PBS before mixing (1×10^4/well) with effector cells in round-bottomed 96-well plates at different E:T ratios (1.25:1, 2.5:1, 5:1, 10:1, 20:1) in triplicates. After 4 h incubation, cell-free supernatants were collected and radioactivity measured by MicroBeta counter (Wallac). The percentage of lysis is calculated by (sample release − spontaneous release)/(maximum release − spontaneous release).

Statistical analysis

The results are expressed as the means ± SEM. Statistical significance was determined using the nonparametric Mann–Whitney *U* test, and differences were considered to be statistically significant when $p < 0.05$.

Results

NK cell depletion induces the early onset of colitis in naive T cell-transferred $RAG^{-/-}$ mice

It has been reported that NK cells suppress the severity of inflammatory diseases such as EAE and colitis (22, 24). NK cells were depleted in the latter colitis study by injection of anti-NK1.1 or anti-ASGM1 Abs, or by the use of a perforin-deficient animal. That study suggested that NK cells may possibly have cytolytic activity for colitogenic $CD4^+$ T_{EM} in this model since knockout of the perforin gene resulted in exacerbation of disease severity. However, it is unclear which stage in the development of colitis is affected by NK cells. Therefore, we first assessed the effect of NK cell depletion at different time points in the development of chronic colitis.

To examine the effect of NK cells in the development of chronic inflammation in the colon, an animal model of colitis was induced by adoptive transfer of $CD4^+CD62L^+D44^-$ (naive) T cells derived from WT SP into $RAG^{-/-}$ recipient mice (2, 3). NK cells were depleted by i.p. injection of the anti-ASGM1 Ab (or vehicle control [PBS]) every other day for 12 wk starting from the day before naive T cell transfer (Fig. 1A). Additionally, some groups were injected with the anti-ASGM1 Ab for 4 wk followed by vehicle control for 8 wk (Fig. 1A), or with the vehicle control for 4 wk followed by 8 wk anti-ASGM1 Ab (Supplemental Fig. 1). Mice injected with the anti-ASGM1 Ab for 12 wk, or for just the first 4 wk, started to show wasting earlier than the vehicle control group that was injected for 12 wk (Fig. 1B). Alternatively, mice injected with vehicle control for 4 wk followed by 8 wk anti-ASGM1 Ab showed a similar wasting curve to that of mice injected with vehicle control for 12 wk (data not shown), suggesting that NK cell depletion at the later stage of colitis induction does not affect the severity of colitis.

However, there was no significant difference in clinical scores between these groups 12 wk after the T cell transfer (Fig. 1C), and all mouse groups showed a similar degree of colitis with thickening and shortening of the colon as well as splenomegaly when sacrificed (Fig. 1D). Consistent with this finding, microscopic evaluation of each group showed similar histopathological features such as wall thickening of the colon, infiltration mainly by mononuclear cells, crypt abscesses, crypt elongation, a decrease in goblet cells, and epithelial damage (Fig. 1E, 1F). Moreover, the production of proinflammatory cytokines by colonic LP T cells isolated from each group was similar (Fig. 1G).

However, there was concern that anti-ASGM1 Ab treatment at an early stage may affect the colitis severity in the $RAG^{-/-}$ mice receiving naive T cells, since the groups with the Ab treatment at an early stage for 4 wk and 12 wk started to exhibit wasting earlier than the control group without the Ab treatment (Fig. 1B). Therefore, we examined these mice at a relatively early time and, interestingly, we found that the Ab-treated group showed significantly more severe colitis in clinical and histological scores compared with the control group 6 wk after T cell transfer (Fig. 2). These data indicate that NK cell depletion affects the early stage of colitis development.

$CD62L^-CD44^+$ and $CD62L^-CD44^-$ T cell subsets are increased by NK cell depletion in naive T cell-reconstituted $RAG^{-/-}$ recipient mice

Because the exacerbation at an early stage of colitis development was observed following NK cell depletion, we assessed the number of $CD4^+$ T cells in SPL and MLN of naive T cell-receiving $RAG^{-/-}$ mice treated with or without the anti-ASGM1 Ab. As seen in Fig. 3A and 3B, increased numbers of T cells were detected, especially

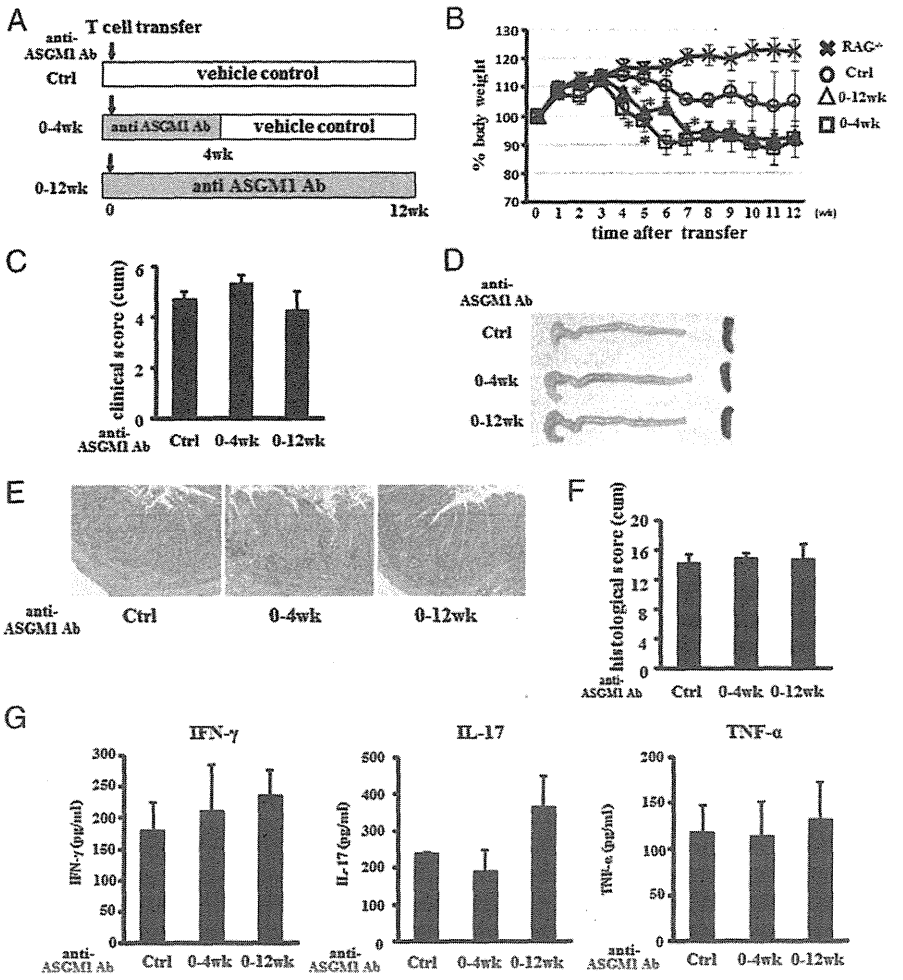

FIGURE 1. NK cell depletion at the early stage of colitis induction in $RAG^{-/-}$ mice results in wasting disease. (**A**) Protocol for NK cell depletion in a chronic colitis setting. $RAG^{-/-}$ mice were injected with either 0.25 mg/mouse anti-ASGM1 Ab (0–12 wk) or vehicle control (Ctrl) every second day for 12 wk from the day before adoptive transfer of naive T cells, or were injected with anti-ASGM1 Ab for 4 wk followed by vehicle control injection for 8 wk (0–4 wk). (**B**) Wasting, as defined by percentage of initial body weight, in $RAG^{-/-}$ mice induced colitis. Mice were injected with naive T cells and either vehicle control for 12 wk (Ctrl, ○), anti-ASGM1 Ab for 12 wk (0–12 wk, △), or anti-ASGM1 Ab for 4 wk followed by 8 wk vehicle control (0–4 wk, □). The non–T cell-injected control group is also shown ($RAG^{-/-}$, cross). Data are expressed as means ± SEM from four mice. $*p < 0.05$. (**C**) Clinical scores of each group are shown. Data are expressed as means ± SEM from four mice. (**D**) Gross appearance of colons (*left*) and SP (*right*) from naive T cell-transferred $RAG^{-/-}$ recipients injected with either vehicle control for 12 wk (Ctrl, *top*), anti-ASGM1 Ab for 4 wk and then control for 8 wk (0–4 wk, *middle*), or anti-ASGM1 Ab for 12 wk (0–12 wk, *bottom*). Representative features from four experiments are shown. (**E**) Histological feature of colons from naive T cell-transferred $RAG^{-/-}$ recipients injected with control for 12 wk (Ctrl, *left*), anti-ASGM1 Ab for 4 wk and then control for 8 wk (0–4 wk, *middle*), or anti-ASGM1 Ab for 12 wk (0–12 wk, *right*). Representative features from each group are shown. (**F**) Histological scores of each group are shown. Data are expressed as means ± SEM from four mice. (**G**) Cytokine production by LP T cells from each group is shown. Concentrations of IFN-γ (*left*), TNF (*middle*), and IL-17 (*right*) in the culture supernatant were measured using ELISA. Data are indicated as means ± SEM from four samples.

in the SPL, within a week after naive T cell injection. Moreover, treatment with the anti-ASGM1 Ab revealed a significantly increased number of T cells in SPL and MLN (Fig. 3A, 3B). Thus, we next determined the development of T_{EM} in these mice by assessment of the expression levels of CD62L and CD44 on T cells. From day 1 to day 3, most T cells still expressed CD62L, but not CD44, regardless of anti-ASGM1 Ab treatment. Interestingly, a $CD62L^{-}CD44^{-}$ subset had appeared in both SPL and MLN by day 5 after treatment with anti-ASGM1 Ab (Fig. 3C–F). This unique T cell subset was significantly increased in the naive T cell-receiving $RAG^{-/-}$ mice treated with anti-ASGM1 Ab, especially in MLN, on days 5 and 7 (Fig. 3F), suggesting that NK cells target this $CD62L^{-}CD44^{-}$ T cell subset upon development of colitogenic $CD62L^{-}CD44^{+}$ T_{EM}.

It is thought that the T_{EM}, but not a naive T cell subset, is targeted by NK cells to regulate excessive immune responses (23, 28). However, our observation indicated that a $CD62L^{-}CD44^{-}$ T cell subset is increased in the absence of NK cells. Therefore, we next assessed the expression levels of several markers, which are associated with NK cell function, on each of the T cell subsets. Splenic $CD62L^{+}CD44^{-}$ (naive, R1; Fig. 4, *left panel*), $CD62L^{-}CD44^{-}$ (R2), and $CD62L^{-}CD44^{+}$ (effector memory, R3) T cell subsets were isolated for FACS analysis from $RAG^{-/-}$ mice that had received naive T cells 5 d previously with anti-ASGM1 Ab treatment the day before T cell reconstitution. The expression of Fas and DR5 in $CD62L^{-}CD44^{+}$ cells was higher than that in $CD62L^{+}CD44^{-}$ T cells (Fig. 4). Interestingly, the expression levels of Fas and DR5 in $CD62L^{-}CD44^{-}$ cells were similar to those of $CD62L^{+}CD44^{-}$, but not of $CD62L^{-}CD44^{+}$. Additionally, the expression level of Qa-1 was similar for all of these T cell subsets (Fig. 4). Furthermore, the expression level of IL-7R/CD127 in $CD62L^{-}CD44^{+}$ cells was similar to that of $CD62L^{+}$

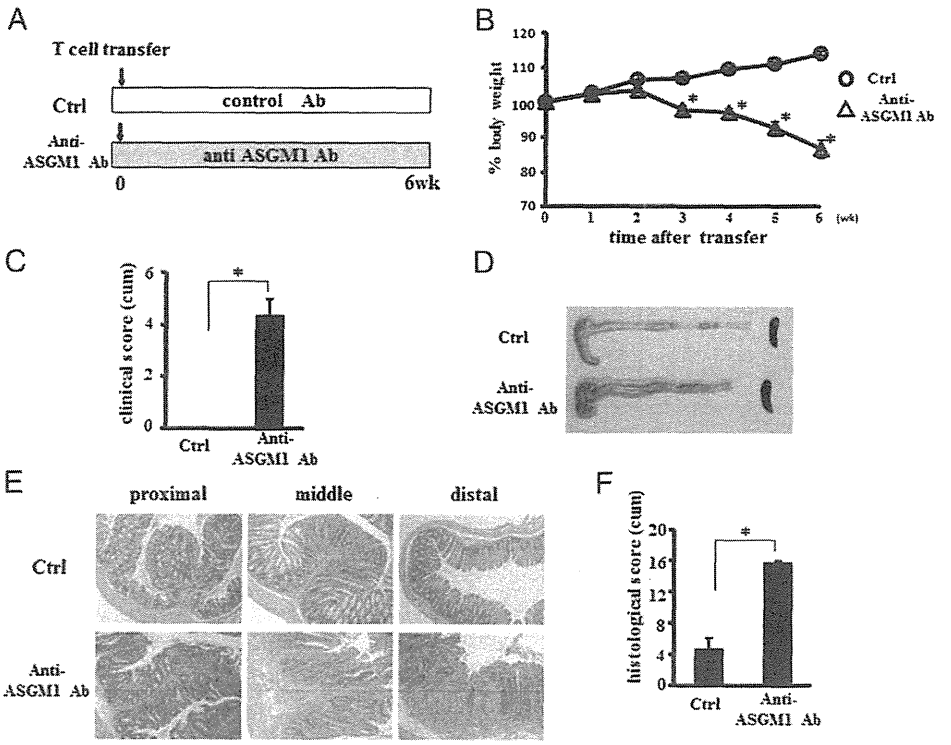

FIGURE 2. NK cell depletion in $RAG^{-/-}$ recipients results in early onset colitis development. (**A**) Protocol for NK cell depletion in a chronic colitis setting. $RAG^{-/-}$ mice were injected with either 0.25 mg/mouse anti-ASGM1 Ab or control IgG every second day for 6 wk from the day before adoptive transfer of naive T cells. (**B**) Wasting, as defined by percentage of initial body weight, in $RAG^{-/-}$ mice induced colitis. Mice were injected with naive T cells with either control IgG (○) or anti-ASGM1 Ab (△) for 6 wk. Data are expressed as means ± SEM from four mice. $*p < 0.05$. (**C**) Clinical scores of each group are shown. Data are expressed as means ± SEM from four mice. $*p < 0.05$. (**D**) Gross appearance of colons (*left*) and SP (*right*) from naive T cell-transferred $RAG^{-/-}$ recipients injected with either control IgG (*top*) or anti-ASGM1 Ab for 6 wk (*bottom*). Representative features from four experiments are shown. (**E**) Histological feature of proximal (*left*), middle (*middle*), and distal (*right*) colons from naive T cell-transferred $RAG^{-/-}$ recipients injected with either control IgG (*top*) or anti-ASGM1 Ab for 6 wk (*botttom*). Representative features from each group are shown. (**F**) Histological scores of each group are shown. Data are expressed as means ± SEM from four mice. $*p < 0.005$.

$CD44^-$ cells. Most $CD62L^-CD44^-$ cells showed a similar IL-7R/CD127 expression level to the other subsets; however, some cells within this subset showed a lower expression of the IL-7R as seen in Fig. 4 (arrow). These results indicate that the mechanism by which NK cells suppress $CD62L^-CD44^-$ T cells may be different from that by which they suppress T_{EM}, which is due to NK cell-induced apoptosis via Fas and/or DR5.

The lack of IL-7 does not affect the cytotoxic activity of NK cells

Because we have previously observed the upregulated annexin V and downregulated Bcl-2 expressions in the $CD4^+$ T cells transferred into $IL\text{-}7^{-/-}RAG^{-/-}$ recipients (10), we speculated that the ability of NK cells to suppress the T cells could be affected by the presence or absence of IL-7. We therefore performed a cytotoxicity assay to test this hypothesis. As expected, NK cells (effector) had negligible cytotoxicity toward $CD62L^+CD44^-$ naive T cells (target) derived from WT SP (T:E ratio, 1:5) regardless of whether rIL-7 was present (Fig. 5A). When $CD62L^-CD44^+$ T_{EM} derived from colonic LP of $RAG^{-/-}$ mice, which had been injected with naive T cells 12 wk previously, were coincubated with the NK cells (T:E ratio, 1:5), the mortality of the target cells was elevated but this cell-mediated cytotoxicity did not change in the presence of rIL-7 (Fig. 5B). These results suggested that the cytotoxic ability of NK cells derived from WT mice was not affected by IL-7 and further suggested that the susceptibility of T cells to the cytotoxic activity of NK cells was not changed by the presence of IL-7 using this assay. When increasing the ratio of $CD62L^-CD44^+$ T_{EM} (T:E ratio, 1:5 to 1:0.6), the mortality was decreased (Fig. 5C). These data suggest that the cytotoxicity is decreased when the number of target T cells exceeds the capacities of effector NK cells to suppress T cells. However, it was still unclear whether the cytotoxic ability of NK cells could be modulated during its development in vivo in the presence or absence of IL-7. Therefore, the cytotoxic ability of NK cells derived from $RAG^{-/-}$ and $IL\text{-}7^{-/-}$ $RAG^{-/-}$ mice was examined. As seen in Fig. 5D, there was little mortality of $CD62L^+$ $CD44^-$ naive T cells alone, and this mortality was unaffected even if coincubated with NK cells derived from either $RAG^{-/-}$ or $IL\text{-}7^{-/-}RAG^{-/-}$ mice (T:E ratio, 1:5). The mortality of $CD62L^-CD44^+$ T_{EM} was elevated compared with that of T_{EM} alone when coincubated with NK cells derived from $RAG^{-/-}$ mice and was similar to that following coincubation with NK cells derived from $IL\text{-}7^{-/-}RAG^{-/-}$ mice (T:E ratio, 1:5; Fig. 5E).

Additionally, the expression levels of NK receptors (30) that reflect the function of NK cells (Fig. 5F), as well as the levels of CD11b and CD27 that determine the differentiation status of NK cells (31) (Fig. 5G), were not altered in NK cells derived from $IL\text{-}7^{-/-}RAG^{-/-}$ mice, compared with those from $RAG^{-/-}$ mice.

To further demonstrate that there are no differences of NK cell functions between $RAG^{-/-}$ and $IL\text{-}7^{-/-}RAG^{-/-}$, we also measured the cytotoxic activities of these cells against YAC-1 cells using the [^{51}Cr] release assay, as well as the production of IFN-γ from these cells. As seen in Fig. 5H and 5I, neither the cytotoxicities against YAC-1 cells nor IFN-γ production of NK cells was modified in the $IL\text{-}7^{-/-}RAG^{-/-}$ mice when compared with

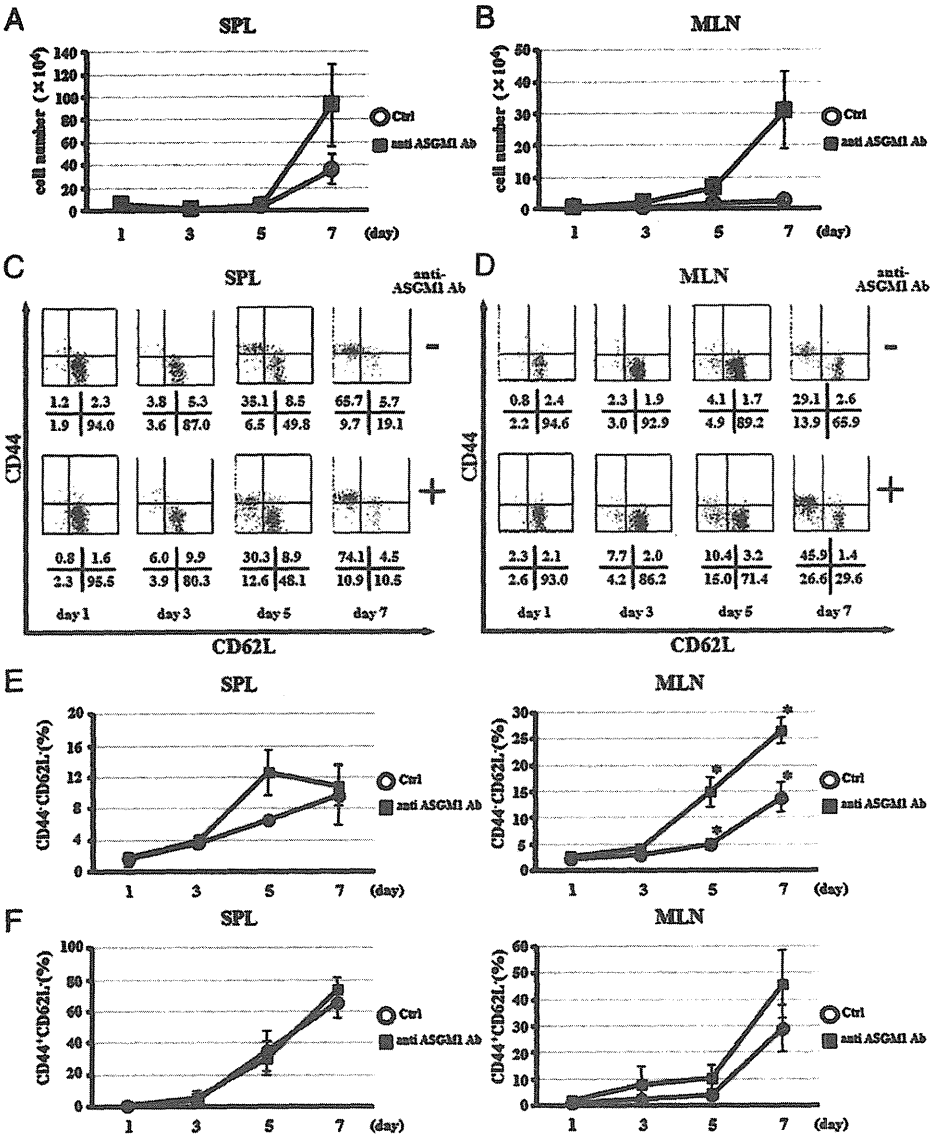

FIGURE 3. NK cell depletion results in the increase in $CD44^+CD62L^-$ and $CD44^-CD62L^-$ subsets in naive T cell-transferred $RAG^{-/-}$ mice. (A and B) Naive T cells derived from WT SP were adoptively transferred into $RAG^{-/-}$ mice that were preinjected with either vehicle control (○) or anti-ASGM1 Ab (■). Mice were sacrificed and the total number of $CD4^+$ T cells isolated from SP (A) or MLN (B) was counted. Cells were stained with PerCP-conjugated anti-CD3 and allophycocyanin-conjugated anti-CD4 Abs, and were then subjected to FACS to calculate the number of T cells in each sample. The number of $CD4^+$ T cells at the indicated time points is shown. Data are expressed as means ± SEM ($n = 4$). (C and D) The naive T cell-receiving $RAG^{-/-}$ mice that had been preinjected with either vehicle control or anti-ASGM1 Ab were sacrificed at the indicated time points after naive T cell transfer. The isolated lymphocytes from SP (C) or MLN (D) were stained with allophycocyanin-conjugated anti-CD4, PerCP-conjugated anti-CD3, FITC-conjugated anti-CD62L, and PE-conjugated anti-CD44 Abs and were subjected to FACS. Representative data from four experiments are shown. The numbers in each data quadrant indicate percentage of gated populations. (E and F) The percentage of $CD44^-CD62L^-$ cells in $RAG^{-/-}$ mice that received naive T cells with or without anti-ASGM1 Ab injection. Mice were sacrificed at the indicated time points, lymphocytes isolated from SP (E) or MLN (F) were stained with anti-CD3, anti-CD4, anti-CD62L, and anti-CD44 Abs and were then subjected to FACS to analyze the percentage of the subset. Data are expressed as means ± SEM from five experiments. $*p < 0.05$.

$RAG^{-/-}$ mice. These results confirm that a lack of IL-7 does not affect the cytotoxic activity of NK cells either in vitro or in vivo.

K cell depletion elicits severe colitis in naive T cell-transferred IL-$7^{-/-}$ $RAG^{-/-}$ recipient mice

We previously reported that the development of colitis is abrogated by a lack of IL-7. Given that NK cells can suppress T cells in vitro and in vivo independently of IL-7, we next assessed the influence of NK cells on colitis in the context of IL-7 deficiency in vivo. IL-$7^{-/-}$ $RAG^{-/-}$ mice were injected i.p. with naive T cells with or without anti-ASGM1 Ab treatment, and colitis was monitored after 12 wk (Fig. 6A). As previously observed, the induction of colitis was completely abrogated in vehicle control-injected IL-$7^{-/-}RAG^{-/-}$ mice, as shown by clinical and histological scores and cytokine production from colonic LP lymphocytes, although the presence of occasional leukocytes was observed in colonic tissues (Fig. 6B–E). However, when anti-ASGM1 Ab was injected, IL-$7^{-/-}RAG^{-/-}$ mice showed elicitation of colitis and similar severity of clinical phenotypes, such as wasting and diarrhea, as did the groups of $RAG^{-/-}$ recipients with or without anti-ASGM1 Ab treatment (Fig. 6B). Consistent with these findings, a significant deterioration in histological findings, such as mucosal damage, cell infil-

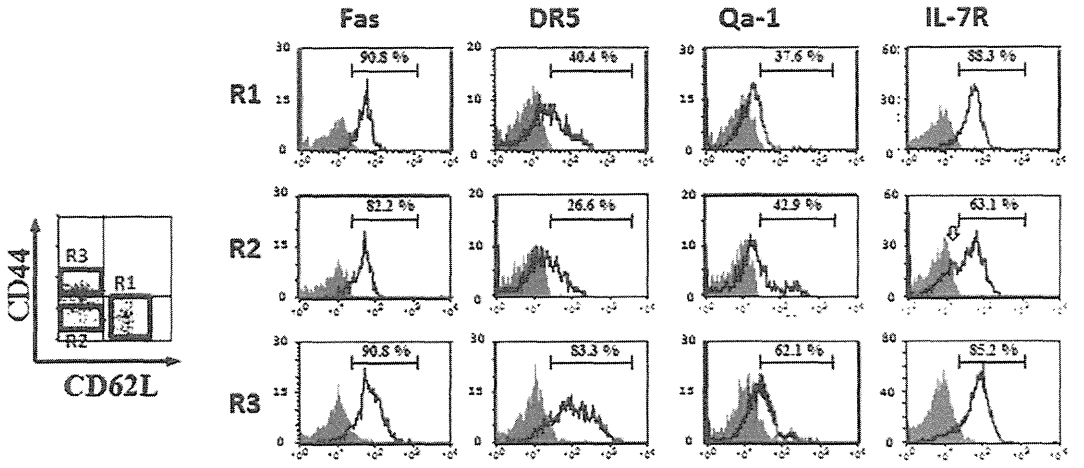

FIGURE 4. NK cells may target the CD62L$^-$CD44$^-$ subset by a different mechanism from that by which they target the CD62L$^-$CD44$^+$ subset. RAG$^{-/-}$ mice preinjected with anti-ASGM1 Ab were sacrificed 5 d after naive T cell transfer. Isolated splenocytes were stained with anti-CD62L, anti-CD44, and either anti-Fas, anti-DR5, anti-Qa1, or anti-CD127 Abs (open histograms) or isotype-matched control (filled histograms) and were then subjected to FACS. The populations within the appropriate gate on forward scatter and side scatter and either CD62L$^+$CD44$^-$ (naive, R1), CD62L$^-$CD44$^-$ (R2) or CD62L$^-$CD44$^+$ (T_{EM}, R3) were analyzed. Representative data from three experiments are shown.

tration, and crypt abscesses, was also observed in IL-7$^{-/-}$RAG$^{-/-}$ mice when treated with anti-ASGM1 Ab (Fig. 6C, 6D) in association with the exacerbation in the clinical scores of these mice. Moreover, the production of cytokines such as IFN-γ, TNF-α, and IL-17 by colonic LPL from anti-ASGM1 Ab-treated IL-7$^{-/-}$ RAG$^{-/-}$ mice was significantly upregulated when compared with the vehicle control-treated group, despite the fact that their production was relatively lower than that of RAG$^{-/-}$ groups with or without anti-ASGM1 Ab treatment (Fig. 6E). These results suggest that severe inflammation occurs in colonic tissues following NK cell depletion even in IL-7$^{-/-}$RAG$^{-/-}$ mice.

Additionally, to confirm the activities of cells that had infiltrated the tissues, absolute numbers of splenic and colonic LP CD4$^+$ T cells isolated from these colitic mice were calculated (Fig. 7A) and analyzed by FACS (Fig. 7B, 7C). As seen in Fig. 7B and 7C, the percentage of NK1.1$^+$ cells in both SP and colonic LP was greatly decreased in T cell-reconstituted mice treated with anti-ASGM1 Ab. Note that the percentages of NK1.1$^+$ populations in both SP and colonic LP from T cell-reconstituted IL-7$^{-/-}$RAG$^{-/-}$ mice not treated with the anti-ASGM1 Ab were dramatically increased, because there were less CD4$^+$ T cells in the tissues (Fig. 7A). Additionally, CD4$^+$ T cells with a CD44$^+$CD62L$^-$ phenotype were observed in all mouse groups (Fig. 7B, 7C). However, the percentage of these cells was lower, especially in colonic LP, in IL-7$^{-/-}$RAG$^{-/-}$ recipient mice not treated with the anti-ASGM1 Ab relative to the other groups. Associated with this finding, the expression levels of IL-7R and CD69 in both splenic and colonic LP CD4$^+$ T cells from IL-7$^{-/-}$RAG$^{-/-}$ recipient mice not treated with the anti-ASGM1 Ab were downregulated relative to the other groups (Fig. 7B, 7C). However, treatment with the anti-ASGM1 Ab resulted in an increase in CD4$^+$CD44$^+$CD62L$^-$ T cells in both splenic and colonic LP, as well as upregulation of the expression of IL-7R and CD69 in IL-7$^{-/-}$RAG$^{-/-}$ recipient mice. These results indicate that the T cells reconstituted into IL-7$^{-/-}$RAG$^{-/-}$ recipient mice are still able to survive even 12 wk after injection, but that they somehow fail to differentiate sufficiently to induce colitis. Moreover, these data suggest that the depletion of NK cells in this context may assist the T cells to establish themselves as pathogenic T cells.

To further confirm whether such elicitation of pathogenic T cells in IL-7$^{-/-}$RAG$^{-/-}$ recipients was induced by NK cell depletion, anti-NK1.1 Ab was used for the same model. IL-7$^{-/-}$RAG$^{-/-}$ mice were injected i.p. with naive T cells with or without anti-NK1.1 Ab treatment, and colitis was monitored after 12 wk (Fig. 8A). The IL-7$^{-/-}$RAG$^{-/-}$ recipients injected with anti-NK1.1 Ab showed severe colitis (Fig. 8B–D) with increased production of proinflammatory cytokines by the colonic LPL when compared with the isotype control-injected mice (Fig. 8E). These results suggested that the phenotypes shown in IL-7$^{-/-}$RAG$^{-/-}$ recipients may reflect NK cell regulation of T cell development in this model.

NK cell depletion at an early stage is critical for the induction of colitis in naive T cell-transferred IL-7$^{-/-}$RAG$^{-/-}$ recipient mice

Because NK cell depletion resulted in the exacerbation of colitis even in IL-7$^{-/-}$RAG$^{-/-}$ recipient mice, we finally examined the effect of NK cell depletion at early and late stages of colitis development in IL-7$^{-/-}$RAG$^{-/-}$ recipient mice. Mice receiving naive T cells were also injected every 48 h with either the vehicle control for 12 wk (Ctrl), anti-ASGM1 Ab for 12 wk (0–12 wk), anti-ASGM1 Ab for 4 wk followed by vehicle control for 8 wk (0–4 wk), or vehicle control for 4 wk followed by 8 wk anti-ASGM1 Ab (4–12 wk), and colitis was monitored after 12 wk (Fig. 9A). Mice injected with anti-ASGM1 Ab for the first 4 wk, or for the entire 12 wk, showed significantly more severe clinical phenotypes of colitis than did the other groups (Fig. 9B), which was associated with thickening and shortening of the colon and splenomegaly (Fig. 9C). Severe inflammation of the colon, as judged by histological analysis, was also noticeably induced in these two groups (Fig. 9D, 9E). However, mice injected with the anti-ASGM1 Ab at a later stage failed to induce colitis, although minor clinical symptoms and infiltration of a few cells into the colon were occasionally observed (Fig. 9B–E). Moreover, these degrees of severity of colitis were consistent with cytokine production from colitic LP T cells, since significantly upregulated IFN-γ and TNF-α production was observed in the groups treated with the anti-ASGM1 Ab either at the beginning or throughout the entire period, but not in the group treated with the Ab only at the later stage (Fig. 9F). Note that the level of IL-17 production in mice treated for the entire period with anti-ASGM1 Ab was significantly higher than that of mice treated with the Ab only at the

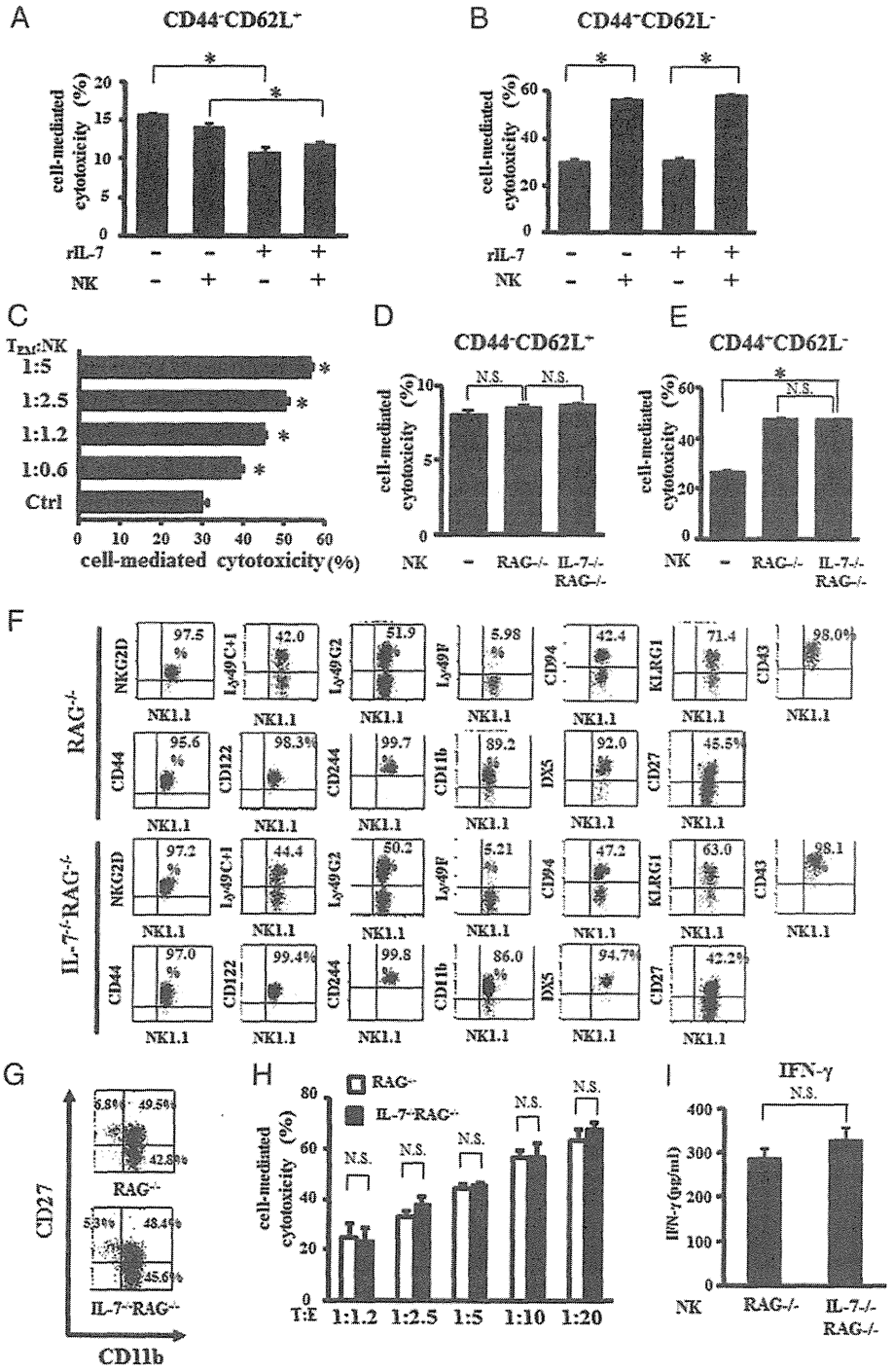

FIGURE 5. Cytotoxic activity of NK cells is not affected in the presence or absence of IL-7. (A–C) Splenic NK cells were isolated from WT mice by FACS sorting. Either $CD4^+CD62L^+CD44^-$ naive T cells isolated from WT SP (A) or $CD4^+CD62L^-CD44^+$ T_{EM} from colonic LP in $RAG^{-/-}$ mice that received naive T cells 12 wk previously (B and C) were stained with PKH2 and cocultured as target (T) cells with the isolated NK cells as effector (E) cells, in the presence or absence of IL-7 for 4 h. Cells were then harvested and stained with PI. The PKH2 and PI double-positive population is assumed to represent dead target cells (28). The mortality of target cells was calculated as the ratio of dead $PKH2^+$ cells. (A) T:E ratio, 1:5, with or without rIL-7; (B) T:E ratio, 1:5, with or without rIL-7; (C) T:E ratio, 1:5, 1:2.5, 1:1.25, or 1:0.625, without rIL-7. Control ($CD4^+$ T cells alone) is also shown as a negative control. Data are expressed as means ± SEM from three experiments. *$p < 0.001$. (D and E) Splenic NK cells were isolated from either $RAG^{-/-}$ or $IL\text{-}7^{-/-}$ $RAG1^{-/-}$ mice by FACS sorting. Either the $CD62L^+CD44^-$ naive T (D) or the $CD62L^-CD44^+$ T_{EM} (E) subset was stained with PKH2 and cocultured for 4 h with splenic NK cells derived from either $RAG^{-/-}$ or $IL\text{-}7^{-/-}RAG1^{-/-}$ mice. Cells were then stained with PI and subjected to the cytotoxic assay described above. Data are expressed as means ± SEM from three experiments. *$p < 0.001$. (F) Splenic NK cells were isolated from $RAG^{-/-}$ and $IL\text{-}7^{-/-}$ $RAG^{-/-}$ mice, and the expression of each NK receptor on these cells was assessed by FACS. The numbers indicate the percentage of cells positive for each NK receptor in the NK1.1-positive population. (G) Splenic NK cells isolated from either $RAG^{-/-}$ or $IL\text{-}7^{-/-}RAG^{-/-}$ mice were stained with anti-CD11b and anti-CD27 Abs and were then subjected to FACS to evaluate their differentiation status. The numbers indicate the quadrant percentages of each differentiation status in the NK1.1-positive population. (H) Splenic NK cells were isolated from $RAG^{-/-}$ (open) and $IL\text{-}7^{-/-}$ $RAG^{-/-}$ (filled) mice by FACS sorting. YAC-1 cells were labeled with $Na_2[^{51}Cr]O_4$ and cocultured as target (T) cells with the isolated NK cells as *(Figure legend continues)*

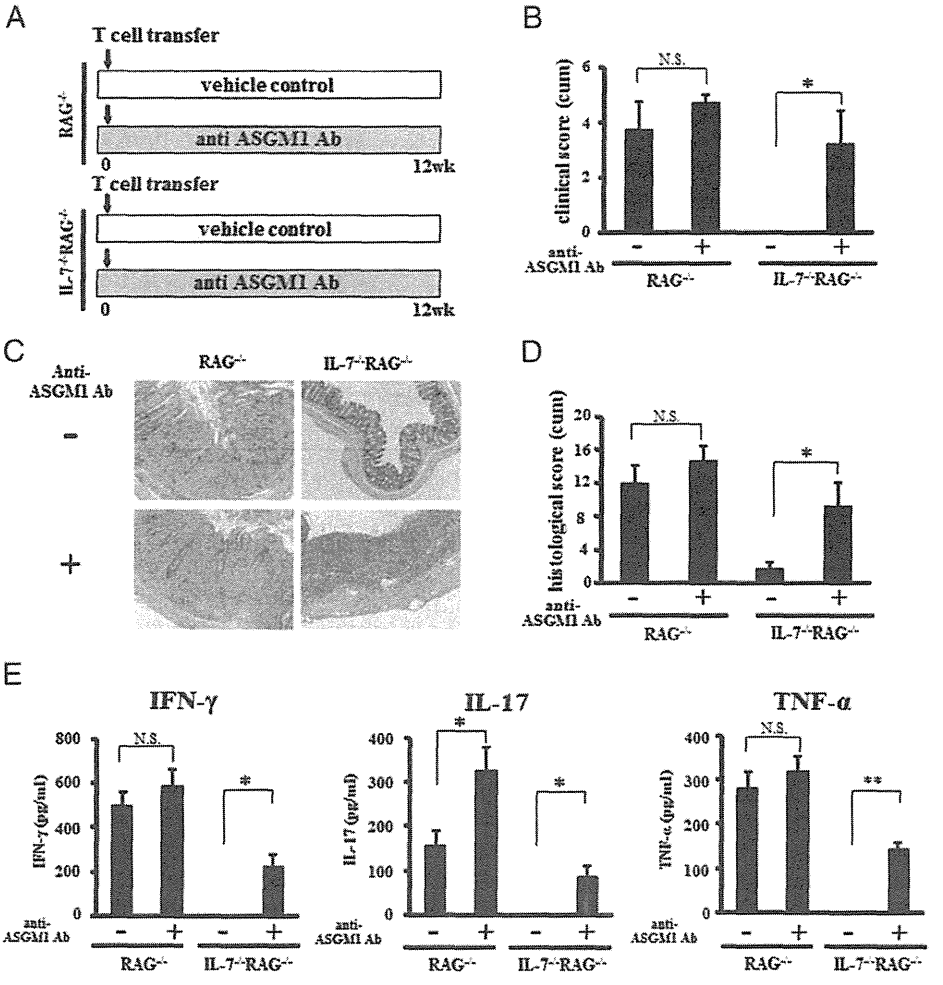

FIGURE 6. NK cell depletion with anti-ASGM1 Ab in naive T cell-receiving IL-$7^{-/-}$$RAG^{-/-}$ mice, as well as in $RAG^{-/-}$ recipients, results in the development of colitis. (**A**) Protocol for NK cell depletion in a colitis setting. Naive T cell-receiving $RAG^{-/-}$ and IL-$7^{-/-}$$RAG^{-/-}$ mice were injected with either anti-ASGM1 Ab (0–12 wk) or vehicle control (Ctrl) every second day for 12 wk starting from the day before adoptive transfer of naive T cells. (**B**) Clinical scores of each group are shown. Data are expressed as means ± SEM from four mice. $*p < 0.05$. (**C**) Histological features of colons from naive T cell-transferred $RAG^{-/-}$ and IL-$7^{-/-}$$RAG^{-/-}$ recipients injected with either vehicle control (Ctrl) or anti-ASGM1 for 12 wk (0–12 wk). Representative features from four experiments are shown. (**D**) Histological scores of each group are shown. Data are expressed as means ± SEM from four mice. $*p < 0.05$. (**E**) Cytokine production by LP T cells from each group is shown. Concentrations of IFN-γ (*left*), TNF (*middle*), and IL-17 (*right*) in the culture supernatant are measured by ELISA. Data are indicated as means ± SEM from four samples. $*p < 0.05$, $**p < 0.01$.

beginning (Fig. 9F), although there was no significant difference in either clinical or histological scores between these groups (Fig. 9B, 9E). These results suggest that NK cell depletion at the early stage, but not the late stage, of T_{EM} development is critical for the induction of colitis in IL-$7^{-/-}$$RAG^{-/-}$ recipient mice.

Discussion

We previously reported that adoptively transferred WT naive T cells injected into IL-$7^{-/-}$$RAG^{-/-}$ mice interestingly failed to induce colitis (10). However, it is known that IL-7 is not required for the in vitro differentiation of naive T cells into Th1 or Th17 cells (12). We therefore speculated that the reason why the IL-$7^{-/-}$$RAG^{-/-}$ mice that received naive T cells failed to maintain colitogenic $CD4^+$ T_{EM} may be associated not only with a lack of IL-7, but also with another mechanism that involves suppression of the primary stage of T_{EM} development in the recipients. We previously reported that apoptosis is preferentially induced in $CD4^+$ T cells when IL-7 is lacking in vivo. Thus, increased numbers of annexin V^+CD4^+ T cells were observed in IL-$7^{-/-}$$RAG^{-/-}$ recipient mice, into which these T cells had been adoptively transferred, compared with $CD4^+$ T cells in $RAG^{-/-}$ recipient mice (10). These data suggested that T cell suppression via apoptosis is a mechanism by which colitis is abrogated in IL-$7^{-/-}$$RAG^{-/-}$ recipient mice. We therefore determined whether NK cells, which are known to induce apoptosis in $CD4^+$ T cells, may play a role in such T cell suppression.

Several reports have suggested that NK cells suppress the inflammation caused by autoimmune responses not only in animal models such as EAE and collagen-induced arthritis, but also in clinical samples from patients with multiple sclerosis and systemic lupus erythematosus in humans (20–22, 28, 32, 33). For example, depletion of NK cells using Abs against NK1.1 or ASGM1 results in disease exacerbation in the EAE model (22, 28). Additionally, it has also been reported that NK cell depletion exacerbates an animal model of colitis, although the details underlying the mechanism have not been elucidated (24).

In the present study, NK cells were depleted in the naive T cell adoptively transferred colitis model to analyze the role of NK cells in this model. $RAG^{-/-}$ and IL-$7^{-/-}$$RAG^{-/-}$ mice that had received naive T cells were depleted of NK cells using an anti-ASGM1 (Figs. 1, 2, 6, 9, Supplemental Figs. 1, 2). However, it was of concern that ASGM1 may be expressed not only in NK cells but also in some subsets of T cells and macrophages when activated (34). Therefore, we also administered anti-NK1.1 Ab

effector (E) cells for 4 h. T:E ratio, 1:20, 1:10, 1:5, 1:2.5, or 1:1.25. Data are expressed as means ± SEM from three experiments. (**I**) Cytokine production by NK cells from each group is shown. Concentrations of IFN-γ in the culture supernatant are measured by ELISA. Data are indicated as means ± SEM from four samples.

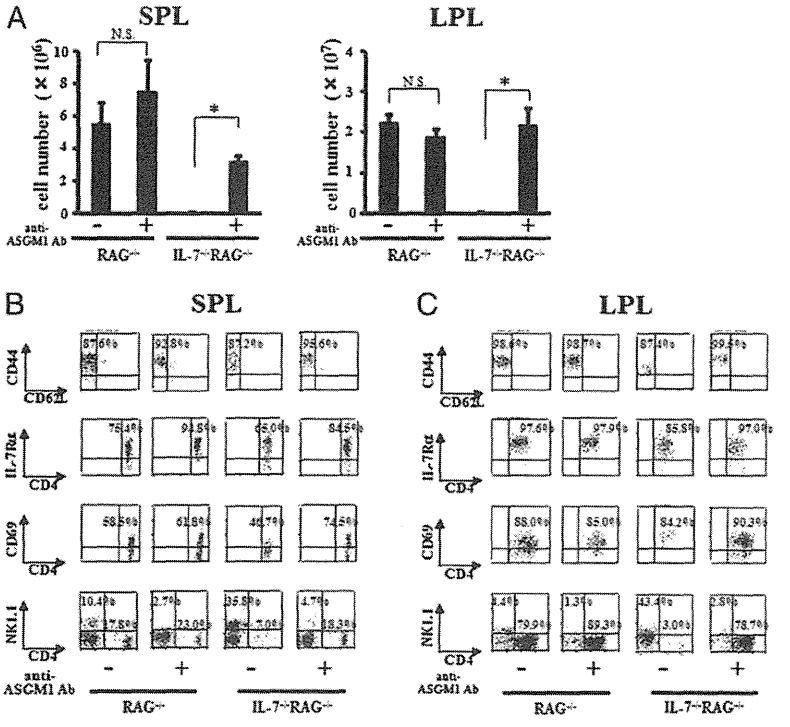

FIGURE 7. Colitogenic T_{EM} are induced in naive T cell-receiving IL-$7^{-/-}$RAG$^{-/-}$ by NK cell depletion. (**A**) Absolute numbers of $CD4^+$ T cells are shown. $CD4^+$ SPL (*left*) or colonic LPL (*right*) were isolated from naive T cell-receiving RAG$^{-/-}$ and IL-$7^{-/-}$ RAG$^{-/-}$ mice injected with either vehicle control (−) or anti-ASGM1 Ab (+) for 12 wk. Data are expressed as means ± SEM from five mice. *$p < 0.001$. (**B** and **C**) Isolated SPL (B) or colonic LPL (C) were stained with anti-CD4 and either anti-CD44, anti-CD127/IL-7Rα, anti-CD69, or anti-NK1.1 Abs and were then subjected to FACS analysis. Representative data from four experiments are shown.

using another experimental approach to confirm that the phenotypes shown in this model were induced by NK cell depletion (Fig. 8). Note that administration of anti-ASGM1 without T cell reconstitution to the IL-$7^{-/-}$RAG$^{-/-}$ mice does not trigger any inflammation in the colon (Supplemental Fig. 2). Also note that the appropriate controls, such as the same amount of rabbit Ig as a control for anti-ASGM1 polyclonal Ab and mouse IgG2a as an isotype-matched control for anti-NK1.1 (PK136), respectively, do not induce colitis in the recipients either (Figs. 2, 8, Supplemental Fig. 2). Interestingly, NK cell depletion at an early stage during colitis induction resulted in exacerbated colitis in the recipient, even in IL-$7^{-/-}$ RAG$^{-/-}$ recipient mice, in association with increased clinical and histological scores as well as upregulated cytokine production by colonic LP T cells. We observed strong

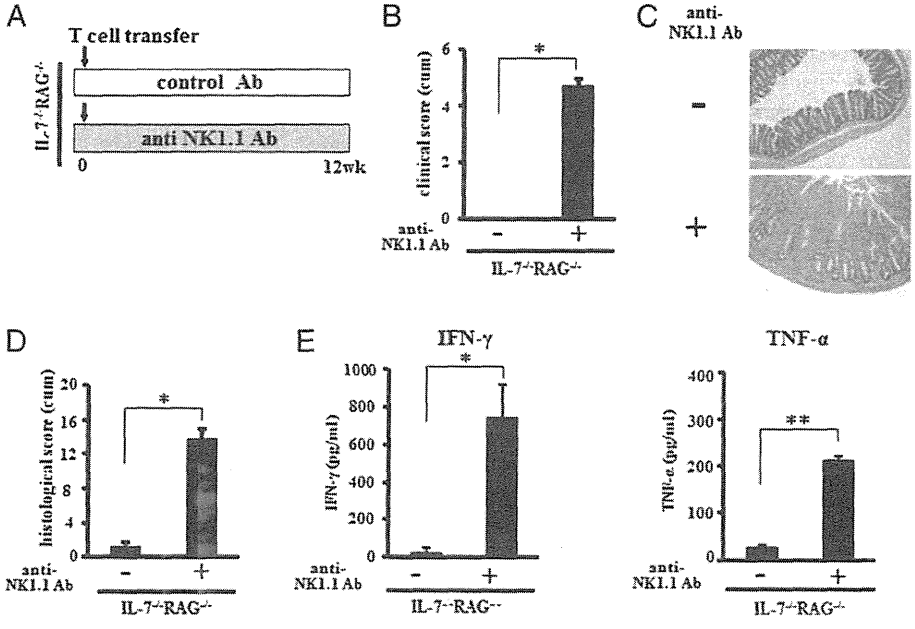

FIGURE 8. NK cell depletion with anti-NK1.1 Ab in naive T cell-receiving IL-$7^{-/-}$RAG$^{-/-}$ mice results in the elicitaion of colitis. (**A**) Protocol for NK cell depletion in a chronic colitis setting. IL-$7^{-/-}$RAG$^{-/-}$ mice receiving naive T cells were injected with either 0.5 mg/mouse anti-NK1.1 Ab or isotype control every second day for 12 wk. (**B**) Clinical scores of each group are shown. Data are expressed as means ± SEM from five mice. *$p < 0.001$. (**C**) Histological feature of colons from naive T cell-transferred IL-$7^{-/-}$RAG$^{-/-}$ recipients injected with isotype control (−, *top*) or anti-NK1.1 Ab (+, *bottom*). Representative features from each group are shown. (**D**) Histological scores of each group are shown. Data are expressed as means ± SEM from five mice. *$p < 0.001$. (**E**) Cytokine production by LP T cells from each group is shown. Concentrations of IFN-γ (*left*) and TNF-α (*right*) in the culture supernatant were measured by ELISA. Data are indicated as means ± SEM from five samples. *$p < 0.05$, **$p < 0.001$.

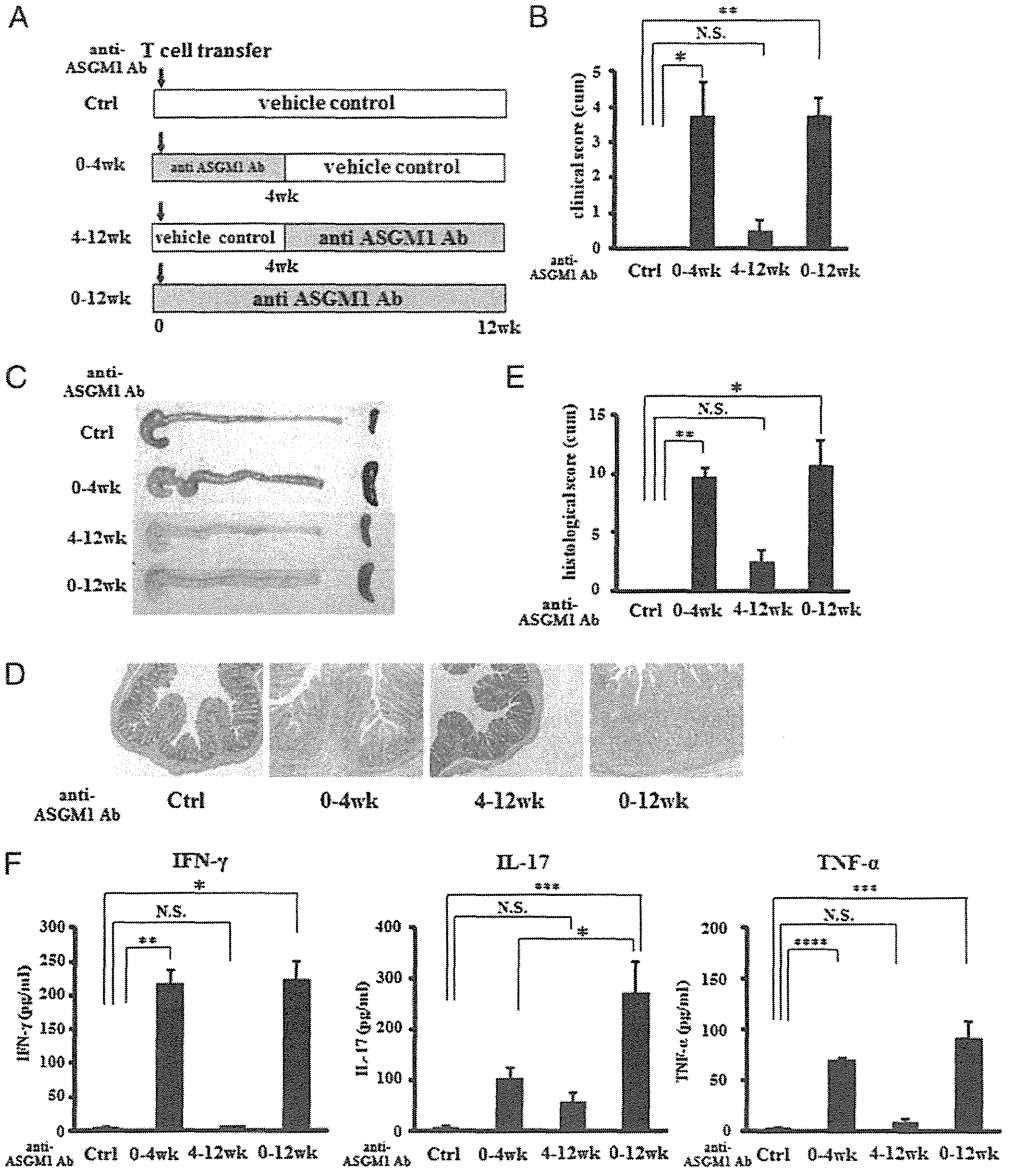

FIGURE 9. NK cell depletion at the early stage, but not at a late stage, in naive T cell-receiving IL-$7^{-/-}$$RAG^{-/-}$ mice results in the elicitation of massive colitis. (**A**) Protocol for NK cell depletion in a setting of chronic colitis. IL-$7^{-/-}$$RAG^{-/-}$ mice were injected with either vehicle control (Ctrl) or anti-ASGM1 Ab (0–12 wk) for 12 wk, anti-ASGM1 Ab for 4 wk followed by vehicle control for 8 wk (0–4 wk), or vehicle control for 4 wk followed by anti-ASGM1 Ab for 8 wk (4–12 wk). (**B**) Clinical scores of each group are shown. Data are expressed as means ± SEM from four mice. $*p < 0.05$, $**p < 0.005$. (**C**) Gross appearance of colons (*left*) and SP (*right*) from naive T cell-transferred IL-$7^{-/-}$$RAG^{-/-}$ recipients injected with either vehicle control for 12 wk (Ctrl), anti-ASGM1 for 4 wk and then vehicle control for 8 wk (0–4 wk), vehicle control for 4 wk and then anti-ASGM1 Ab for 8 wk (4–12 wk), or anti-ASGM1 Ab for 12 wk (0–12 wk). Representative features from four experiments are shown. (**D**) Histological feature of colons from naive T cell-transferred IL-$7^{-/-}$ $RAG^{-/-}$ recipients injected with either control for 12 wk (Ctrl), anti-ASGM1 for 4 wk and then control for 8 wk (0–4 wk), vehicle control for 4 wk and then anti-ASGM1 Ab for 8 wk (4–12 wk), or anti-ASGM1 for 12 wk (0–12 wk). Representative features of each group are shown. (**E**) Histological scores of each group are shown. Data are expressed as means ± SEM from four mice. $*p < 0.05$, $**p < 0.01$. (**F**) Cytokine production by LP T cells from each group is shown. Concentrations of IFN-γ (*left*), TNF (*middle*), and IL-17 (*right*) in the culture supernatant were measured by ELISA. Data are indicated as means ± SEM from four samples. $*p < 0.05$, $**p < 0.01$, $***p < 0.005$, $****p < 0.001$.

infiltration in colonic tissues ~4 wk after the adoptive transfer into $RAG^{-/-}$ recipients (10). We therefore compared the effect of NK cell depletion by treatment with an anti-ASGM1 Ab at early (0–4 wk) or late stages (4–12 wk) after naive T cell transfer to treatment over the entire 12-wk period (0–12 wk) after transfer. Ab treatment at the early stage and over the entire 12 wk resulted in a similar degree of colitis exacerbation whereas Ab treatment at the late stage did not exacerbate colitis (Figs. 1, 9). Such exacerbation of colitis occurred relatively latent in the presence of IL-7 in the $RAG^{-/-}$ compared with the IL-$7^{-/-}$$RAG^{-/-}$ recipients when sacrificed at 12 wk after T cell transfer (Figs. 6, 7). However, the difference of colitis severity in the $RAG^{-/-}$ recipients with or without Ab treatment was interestingly remarkable when sacrificed at 6 wk after T cell receiving (Fig. 2). These results imply that NK cell function is critical for colitogenic T cell suppression at the early stage of colitis development.

Because the $CD4^+CD44^+CD62L^-$ colitogenic T_{EM} in the recipients were suggested to be suppressed at the early stage by NK cells (Figs. 1, 2, 9), we further analyzed the effect of NK cells on the development of $CD4^+$ T cells within a week after recon-

stitution into the $RAG^{-/-}$ recipients (Fig. 3). The number of $CD4^+$ T cells in SPL and MLN was significantly increased 5–7 d after the transfer when NK cells were depleted compared with the control (Fig. 3A, 3B). Additionally, the significant increase of the $CD44^+CD62L^-$ T_{EM} subset was observed at this point when NK cells were depleted. $CD4^+CD44^+CD62L^-$ colitogenic T_{EM} are suggested to be susceptible to cell death when they are activated. We therefore analyzed the expression of several markers characteristic of NK cell targets on the $CD44^+CD62L^-$ T_{EM} subset, such as Fas, DR5, and Qa-1, which are the specific receptors or ligand for Fas ligand, TRAIL, and NKG2A, respectively (Fig. 4). As expected, this T cell subset expresses high levels of Fas and DR5, thereby making them susceptible to apoptosis (20). Additionally, these T cells also express some but not a significant level of Qa-1, which induces inhibitory signaling in NK cells via NKG2A. These data indicate that NK cells may suppress $CD4^+CD44^+CD62L^-$ colitogenic T_{EM} via apoptosis, and consistent with our previous observation of downregulated Bcl-2 and upregulated annexin V in $CD4^+$ T cells by the lack of IL-7 in vivo (10).

Furthermore, we also observed an increased unique T cell subset, $CD44^-CD62L^-$, when NK cells were depleted (Fig. 3C–E). We were able to observe these cells in the SPL and MLN within 2 wk after T cell transfer into RAG mice, and subsequently they were not detectable afterward (Fig. 7B, 7C). The fact that the $CD44^-CD62L^-$ T cell subset was only observed at the beginning of colitogenic T cell development would suggest that this interesting population may be associated with the importance of early stage at the pathogenic T cell development in this chronic colitis model. This T cell subset, which is distinct from $CD44^+CD62L^-$ T_{EM}, is likely to be a second target of NK cells. However, the expressions of Fas and DR5 are lower on these cells compared with those of the $CD44^+CD62L^-$ T_{EM} (Fig. 4). The expression of Qa-1 in $CD44^-CD62L^-$ is not greatly different from that of the $CD44^+CD62L^-$ subset. This phenotype of the $CD44^-CD62L^-$ subset does not suggest that it is a target of NK cells. However, a recent report showed that CD44 expression on Th1 cells is required to prevent apoptosis via Fas signaling (35). Thus, the $CD44^-CD62L^-$ subset may be susceptible to apoptosis, since these cells still express some level of Fas on their surface. This may be one of the reasons why early stage of T cell development in this colitis model is targeted by NK cells. Additionally, this possibility may be a potential reason why Th1 cells fail to survive when transferred into $IL\text{-}7^{-/-}RAG^{-/-}$ mice. It is also possible that NK cells may regulate $CD44^+CD62L^-$ and $CD44^-CD62L^-$ cells by different mechanisms. Analysis of IL-7R expression levels of the $CD44^-CD62L^-$ subset revealed two distinct populations: $IL\text{-}7R^{hi}$ and $IL\text{-}7R^{lo}$ (indicated with an arrow in Fig. 4). The $IL\text{-}7R^{lo}$ population in this subset could potentially arise due to transient downregulation of IL-7R expression during differentiation. Unfortunately, the scarcity of these cells prohibited their further analysis and characterization. However, these cells still need to be further studied.

Our recent studies suggested that $IL\text{-}7^{-/-}RAG^{-/-}$ mice were able to induce colitis when parabiosed with colitic $RAG^{-/-}$ recipient mice that had received naive T cells 6 wk previously (15). Moreover, deparabiosed $IL\text{-}7^{-/-}RAG^{-/-}$mice, which were surgically separated from T cell-receiving $RAG^{-/-}$–$IL\text{-}7^{-/-}RAG^{-/-}$ parabionts 6 wk after the initial surgery, still maintained chronic colitis for at least another 12 wk (16). The latter finding is similar to our present observation that $IL\text{-}7^{-/-}RAG^{-/-}$ recipient mice, which had been depleted of NK cells at an early stage during induction, showed elicited colitis, even after completion of the anti-ASGM1 Ab treatment (Fig. 9). However, the mechanism by which the colitogenic T cells are maintained in the $IL\text{-}7^{-/-}RAG^{-/-}$ mice after the establishment of massive colitis is still unclear. One potential interpretation is that the pathogenic T cells can continue to proliferate, resulting in induction of colitis when the T cell number exceeds the capacity of the NK cells to suppress the T cells. A second possibility is based on the recent report that IL-17 inhibits NK cell-suppressive ability (36). It has been suggested that the increased IL-17 production from T cells that occurs when the severity of the colitis increases may affect NK cell function. The latter possibility is supported by one of our observations that NK cell depletion starting at the late stage of colitis development failed to exacerbate colitis (Supplemental Fig. 1).

We observed that the characteristics of NK cells are not modified by the lack of IL-7 in $RAG^{-/-}$ mice (Fig. 5F). This observation is consistent with a previous report by Vosshenrich et al. (37) showing that the lack of IL-7 does not affect the growth, phenotype, or effector functions of NK cells in vivo, although IL-7 had been reported to influence NK cell differentiation. Consistent with this, we also observed that the differentiation of NK cells, which is characterized by the expression of CD11b and CD27 (31), is not altered in the same mice (Fig. 5G). Additionally, there is no significant difference between NK cells derived from $RAG^{-/-}$ and $IL\text{-}7^{-/-}RAG^{-/-}$ mice in terms of their cytotoxic activities against the target cells such as T cells and YAC-1 cells (Fig. 5D, 5E, 5H) as well as the production of IFN-γ (Fig. 5I). These data indicate that the dramatic difference in the severity of colitis between $IL\text{-}7^{-/-}RAG^{-/-}$ and $RAG^{-/-}$ recipients following NK depletion is not caused by a difference in NK function between NK cells derived from $RAG^{-/-}$ and $IL\text{-}7^{-/-}RAG^{-/-}$ mice.

The $IL\text{-}7^{-/-}RAG^{-/-}$ recipient mice that received naive T cells failed to induce colitis even though the cytotoxicity of NK cells was not altered. One potential explanation of this result is that the susceptibility of T cells to apoptosis is increased in these mice. It has been reported by others that the expression of Bcl-2, an anti-apoptotic molecule, in T cells is downregulated in $IL\text{-}7^{-/-}$ mice (38, 39). We have also reported that Bcl-2 expression is downregulated in T cells injected into $IL\text{-}7^{-/-}RAG^{-/-}$ recipient mice (10). A second explanation is based on our previous report that IL-7 contributes to the expansion of colitogenic T cells (39). Thus, these data suggest that colitogenic T cells are not able to survive in the mice due to their reduced expansion and increased susceptibility to apoptosis at the early stage of colitis development.

In this study, we demonstrate NK cell-mediated regulation of T cell development, which is associated with the pathogenesis of chronic colitis. Although the detailed mechanism still remains to be elucidated, an insight into such a mechanism is significant for understanding the regulation of mucosal immune responses.

Acknowledgments

We are grateful to Dr. R. Zamoyska for providing the IL-7–deficient mice and Drs. M. Yamazaki and T. Tomita for critical discussions.

Disclosures

The authors have no financial conflicts of interest.

References

1. Fujino, S., A. Andoh, S. Bamba, A. Ogawa, K. Hata, Y. Araki, T. Bamba, and Y. Fujiyama. 2003. Increased expression of interleukin 17 in inflammatory bowel disease. *Gut* 52: 65–70.
2. Powrie, F., M. W. Leach, S. Mauze, L. B. Caddle, and R. L. Coffman. 1993. Phenotypically distinct subsets of $CD4^+$ T cells induce or protect from chronic intestinal inflammation in C. B-17 *scid* mice. *Int. Immunol.* 5: 1461–1471.
3. Ostanin, D. V., J. Bao, I. Koboziev, L. Gray, S. A. Robinson-Jackson, M. Kosloski-Davidson, V. H. Price, and M. B. Grisham. 2009. T cell transfer model of chronic colitis: concepts, considerations, and tricks of the trade. *Am. J. Physiol. Gastrointest. Liver Physiol.* 296: G135–G146.

4. Namen, A. E., S. Lupton, K. Hjerrild, J. Wignall, D. Y. Mochizuki, A. Schmierer, B. Mosley, C. J. March, D. Urdal, and S. Gillis. 1988. Stimulation of B-cell progenitors by cloned murine interleukin-7. *Nature* 333: 571–573.
5. Fry, T. J., and C. L. Mackall. 2005. The many faces of IL-7: from lymphopoiesis to peripheral T cell maintenance. *J. Immunol.* 174: 6571–6576.
6. Surh, C. D., O. Boyman, J. F. Purton, and J. Sprent. 2006. Homeostasis of memory T cells. *Immunol. Rev.* 211: 154–163.
7. Watanabe, M., Y. Ueno, T. Yajima, Y. Iwao, M. Tsuchiya, H. Ishikawa, S. Aiso, T. Hibi, and H. Ishii. 1995. Interleukin 7 is produced by human intestinal epithelial cells and regulates the proliferation of intestinal mucosal lymphocytes. *J. Clin. Invest.* 95: 2945–2953.
8. Watanabe, M., Y. Ueno, T. Yajima, S. Okamoto, T. Hayashi, M. Yamazaki, Y. Iwao, H. Ishii, S. Habu, M. Uehira, et al. 1998. Interleukin 7 transgenic mice develop chronic colitis with decreased interleukin 7 protein accumulation in the colonic mucosa. *J. Exp. Med.* 187: 389–402.
9. Yamazaki, M., T. Yajima, M. Tanabe, K. Fukui, E. Okada, R. Okamoto, S. Oshima, T. Nakamura, T. Kanai, M. Uehira, et al. 2003. Mucosal T cells expressing high levels of IL-7 receptor are potential targets for treatment of chronic colitis. *J. Immunol.* 171: 1556–1563.
10. Totsuka, T., T. Kanai, Y. Nemoto, S. Makita, R. Okamoto, K. Tsuchiya, and M. Watanabe. 2007. IL-7 Is essential for the development and the persistence of chronic colitis. *J. Immunol.* 178: 4737–4748.
11. Fujii, T., T. Tomita, T. Kanai, Y. Nemoto, T. Totsuka, N. Sakamoto, T. Nakamura, K. Tsuchiya, R. Okamoto, and M. Watanabe. 2008. FTY720 suppresses the development of colitis in lymphoid-null mice by modulating the trafficking of colitogenic $CD4^+$ T cells in bone marrow. *Eur. J. Immunol.* 38: 3290–3303.
12. Mangan, P. R., L. E. Harrington, D. B. O'Quinn, W. S. Helms, D. C. Bullard, C. O. Elson, R. D. Hatton, S. M. Wahl, T. R. Schoeb, and C. T. Weaver. 2006. Transforming growth factor-β induces development of the T_H17 lineage. *Nature* 441: 231–234.
13. Min, B., H. Yamane, J. Hu-Li, and W. E. Paul. 2005. Spontaneous and homeostatic proliferation of CD4 T cells are regulated by different mechanisms. *J. Immunol.* 174: 6039–6044.
14. Kieper, W. C., A. Troy, J. T. Burghardt, C. Ramsey, J. Y. Lee, H. Q. Jiang, W. Dummer, H. Shen, J. J. Cebra, and C. D. Surh. 2005. Recent immune status determines the source of antigens that drive homeostatic T cell expansion. *J. Immunol.* 174: 3158–3163.
15. Tomita, T., T. Kanai, Y. Nemoto, T. Totsuka, R. Okamoto, K. Tsuchiya, N. Sakamoto, and M. Watanabe. 2008. Systemic, but not intestinal, IL-7 is essential for the persistence of chronic colitis. *J. Immunol.* 180: 383–390.
16. Tomita, T., T. Kanai, T. Totsuka, Y. Nemoto, R. Okamoto, K. Tsuchiya, N. Sakamoto, T. Ohteki, T. Hibi, and M. Watanabe. 2009. IL-7 is essential for lymphopenia-driven turnover of colitogenic $CD4^+$ memory T cells in chronic colitis. *Eur. J. Immunol.* 39: 2737–2747.
17. Vivier, E., E. Tomasello, M. Baratin, T. Walzer, and S. Ugolini. 2008. Functions of natural killer cells. *Nat. Immunol.* 9: 503–510.
18. Cooper, M. A., T. A. Fehniger, A. Fuchs, M. Colonna, and M. A. Caligiuri. 2004. NK cell and DC interactions. *Trends Immunol.* 25: 47–52.
19. Walzer, T., M. Dalod, S. H. Robbins, L. Zitvogel, and E. Vivier. 2005. Natural-killer cells and dendritic cells: "l'union fait la force". *Blood* 106: 2252–2258.
20. Lunemann, A., J. D. Lunemann, and C. Munz. 2009. Regulatory NK-cell functions in inflammation and autoimmunity. *Mol. Med.* 15: 352–358.
21. Takahashi, K., T. Aranami, M. Endoh, S. Miyake, and T. Yamamura. 2004. The regulatory role of natural killer cells in multiple sclerosis. *Brain* 127: 1917–1927.
22. Zhang, B., T. Yamamura, T. Kondo, M. Fujiwara, and T. Tabira. 1997. Regulation of experimental autoimmune encephalomyelitis by natural killer (NK) cells. *J. Exp. Med.* 186: 1677–1687.
23. Lu, L., K. Ikizawa, D. Hu, M. B. Werneck, K. W. Wucherpfennig, and H. Cantor. 2007. Regulation of activated $CD4^+$ T cells by NK cells via the Qa-1-NKG2A inhibitory pathway. *Immunity* 26: 593–604.
24. Fort, M. M., M. W. Leach, and D. M. Rennick. 1998. A role for NK cells as regulators of $CD4^+$ T cells in a transfer model of colitis. *J. Immunol.* 161: 3256–3261.
25. Kasai, M., T. Yoneda, S. Habu, Y. Maruyama, K. Okumura, and T. Tokunaga. 1981. In vivo effect of anti-asialo GM1 antibody on natural killer activity. *Nature* 291: 334–335.
26. Makita, S., T. Kanai, Y. Nemoto, T. Totsuka, R. Okamoto, K. Tsuchiya, M. Yamamoto, H. Kiyono, and M. Watanabe. 2007. Intestinal lamina propria retaining $CD4^+CD25^+$ regulatory T cells is a suppressive site of intestinal inflammation. *J. Immunol.* 178: 4937–4946.
27. Onizawa, M., T. Nagaishi, T. Kanai, K. Nagano, S. Oshima, Y. Nemoto, A. Yoshioka, T. Totsuka, R. Okamoto, T. Nakamura, et al. 2009. Signaling pathway via TNF-α/NF-κB in intestinal epithelial cells may be directly involved in colitis-associated carcinogenesis. *Am. J. Physiol. Gastrointest. Liver Physiol.* 296: G850–G859.
28. Xu, W., G. Fazekas, H. Hara, and T. Tabira. 2005. Mechanism of natural killer (NK) cell regulatory role in experimental autoimmune encephalomyelitis. *J. Neuroimmunol.* 163: 24–30.
29. Slezak, S. E., and P. K. Horan. 1989. Cell-mediated cytotoxicity: a highly sensitive and informative flow cytometric assay. *J. Immunol. Methods* 117: 205–214.
30. Di Santo, J. P. 2006. Natural killer cell developmental pathways: a question of balance. *Annu. Rev. Immunol.* 24: 257–286.
31. Hayakawa, Y., and M. J. Smyth. 2006. CD27 dissects mature NK cells into two subsets with distinct responsiveness and migratory capacity. *J. Immunol.* 176: 1517–1524.
32. Takeda, K., and G. Dennert. 1993. The development of autoimmunity in C57BL/6 lpr mice correlates with the disappearance of natural killer type 1-positive cells: evidence for their suppressive action on bone marrow stem cell proliferation, B cell immunoglobulin secretion, and autoimmune symptoms. *J. Exp. Med.* 177: 155–164.
33. Aranami, T., S. Miyake, and T. Yamamura. 2006. Differential expression of CD11c by peripheral blood NK cells reflects temporal activity of multiple sclerosis. *J. Immunol.* 177: 5659–5667.
34. Wiltrout, R. H., A. Santoni, E. S. Peterson, D. C. Knott, W. R. Overton, R. B. Herberman, and H. T. Holden. 1985. Reactivity of anti-asialo GM1 serum with tumoricidal and non-tumoricidal mouse macrophages. *J. Leukoc. Biol.* 37: 597–614.
35. Baaten, B. J., C. R. Li, M. F. Deiro, M. M. Lin, P. J. Linton, and L. M. Bradley. 2010. CD44 regulates survival and memory development in Th1 cells. *Immunity* 32: 104–115.
36. Kawakami, Y., Y. Tomimori, K. Yumoto, S. Hasegawa, T. Ando, Y. Tagaya, S. Crotty, and T. Kawakami. 2009. Inhibition of NK cell activity by IL-17 allows vaccinia virus to induce severe skin lesions in a mouse model of eczema vaccinatum. *J. Exp. Med.* 206: 1219–1225.
37. Vosshenrich, C. A., T. Ranson, S. I. Samson, E. Corcuff, F. Colucci, E. E. Rosmaraki, and J. P. Di Santo. 2005. Roles for common cytokine receptor gamma-chain-dependent cytokines in the generation, differentiation, and maturation of NK cell precursors and peripheral NK cells in vivo. *J. Immunol.* 174: 1213–1221.
38. Kondrack, R. M., J. Harbertson, J. T. Tan, M. E. McBreen, C. D. Surh, and L. M. Bradley. 2003. Interleukin 7 regulates the survival and generation of memory CD4 cells. *J. Exp. Med.* 198: 1797–1806.
39. Okada, E., M. Yamazaki, M. Tanabe, T. Takeuchi, M. Nanno, S. Oshima, R. Okamoto, K. Tsuchiya, T. Nakamura, T. Kanai, et al. 2005. IL-7 exacerbates chronic colitis with expansion of memory IL-7Rhigh CD4+ mucosal T cells in mice. *Am. J. Physiol. Gastrointest. Liver Physiol.* 288: G745–G754.

Cellular & Molecular Immunology (2012), 1–7

www.nature.com/cmi

REVIEW

Current advances in humanized mouse models

Ryoji Ito, Takeshi Takahashi, Ikumi Katano and Mamoru Ito

Humanized mouse models that have received human cells or tissue transplants are extremely useful in basic and applied human disease research. Highly immunodeficient mice, which do not reject xenografts and support cell and tissue differentiation and growth, are indispensable for generating additional appropriate models. Since the early 2000s, a series of immunodeficient mice appropriate for generating humanized mice has been successively developed by introducing the *IL-2Rγ*^{null} gene (e.g., NOD/SCID/γc^{null} and Rag2^{null}γc^{null} mice). These strains show not only a high rate of human cell engraftment, but also generate well-differentiated multilineage human hematopoietic cells after human hematopoietic stem cell (HSC) transplantation. These humanized mice facilitate the analysis of human hematology and immunology *in vivo*. However, human hematopoietic cells developed from HSCs are not always phenotypically and functionally identical to those in humans. More recently, a new series of immunodeficient mice compensates for these disadvantages. These mice were generated by genetically introducing human cytokine genes into NOD/SCID/γc^{null} and Rag2^{null}γc^{null} mice. In this review, we describe the current knowledge of human hematopoietic cells developed in these mice. Various human disease mouse models using these humanized mice are summarized.
Cellular & Molecular Immunology advance online publication, 13 February 2012; doi:10.1038/cmi.2012.2

Keywords: animal model; immunodeficient mice; immunology; hematology; humanized mice

INTRODUCTION

'Humanized' mouse models in which various types of human cells and tissues are engrafted and function, as they would in humans are considered extremely useful in basic and applied human disease research.[1–4] For this purpose, highly immunodeficient mice, which do not reject xenografts and support the differentiation and growth of cells and tissues, are indispensable. The support system that maintains human cells and tissues is also a key factor. In addition, technical modifications necessary for the generation of humanized mice are important.

The discoveries of nude and severe combined immunodeficiency (SCID) mice were key advances in the development of immunodeficient mice for xenotransplantation.[5,6] The development of non-obese diabetic (NOD)/SCID mice *via* the introduction of the *Prdkc*^{scid} gene into a NOD inbred strain also contributed to the generation of humanized mice.[7,8] NOD/SCID/β2m^{null} and NOD/Rag1^{null}Pfp^{null} mice were subsequently derived from NOD/SCID and NOD/Rag1^{null} mice.[9,10]

Since the early 2000s, immunodeficient mice appropriate for generating humanized mice have been successively developed by introducing the mutant *IL2rγ* gene into NOD/SCID and RAG1/2^{null} mice by backcross mating, thus resulting in NOD/SCID/γc^{null} mice[11,12] and Rag1/2^{null}γc^{null} mice.[13–16] These mice show multiple immunodeficiencies, including defects in T, B and natural killer (NK) cells, and reduced macrophage (Mϕ) and dendritic cell (DC) function.[11] In these mice, extremely high human cell engraftment rates and increases in well-differentiated human multilineage hematopoietic cells from human hematopoietic stem cells (HSCs), as compared with parent immunodeficient mice, were observed.[17–19] Humanized mice that retain various human immune cells are often termed human immune system mice[3] or human hematolymphoid system mice.[20] The production of humanized mice that are reconstructed with human cells would facilitate analysis of the underlying mechanisms of human disease pathogenesis. Indeed, various humanized models have been developed using these mice.

Various technical modifications have been used when generating humanized mice. These include modifications in the HSC injection route, age of mice, and HSC and irradiation sources, each of which may affect the efficacy of human cell engraftment. In terms of the injection route and age, intrahepatic or intravenous injection (through the facial vein) into newborn mice and intravenous injection (*via* the tail vein) into adult mice were generally used.[11,14,21] Brehm *et al.*[16] examined various parameters, including injection route, injection age and immunodeficient mouse strains. By comparing engraftment rates of human cells from HSCs, they concluded that intrahepatic injection of HSCs into newborn mice enhanced engraftment as compared with adult mice. With respect to the source of HSCs, CD34$^+$ cells from cord blood or fetal liver were typically used. However, CD34$^+$ cells from granulocyte colony-stimulating factor (G-CSF) mobilized peripheral blood (PB) or bone marrow (BM) served as additional sources. Lepus *et al.*[22] reported that CD34$^+$ cells from fetal liver were more efficient than those from cord blood or G-CSF-mobilized PB. In addition, Matsumura *et al.*[23] reported that CD34$^+$ cells from cord blood were more effective than those from G-CSF-mobilized PB and BM. Busulfan treatment can also be used in place of irradiation, and results in more effective differentiation of B cells from HSCs as compared with

Central Institute for Experimental Animals, Kawasaki, Japan
Correspondence: Dr M Ito, Central Institute for Experimental Animals, 3-25-12, Tonomachi, Kawasaki-ku, Kawasaki 210-0821, Japan.
E-mail: mito@ciea.or.jp
Received 10 November 2011; revised 5 January 2012; accepted 10 January 2012

irradiation.[24] The use of this drug would be beneficial for research, since special equipment is not required. The engraftment rate of human cells from HSCs varies between reports. A possible explanation for this difference is the quality of HSCs, which is influenced by different isolation techniques and the HSC source (i.e., cord blood or fetal liver).

Despite these efforts, some human cell lineages, such as erythrocytes and neutrophils, have not yet been developed in humanized mice. The differentiation of HSCs into immature human T and B cells and poor interactions between these cells were suggested based on cell phenotype analysis and the rare production of antigen-specific immunoglobulin G (IgG) class antibodies.[25] These results suggest that current immunodeficient mice may be insufficient, and human factors that support the differentiation and maturation of cells and mediate cell-to-cell interactions must be introduced. To this end, a new series of immunodeficient mice has been generated by introducing human cytokine genes into NOD/SCID/γc^{null}, $Rag2^{null}\gamma c^{null}$ mice.

In this review, we describe the current knowledge of human hematopoietic cells developed in NOD/SCID/γc^{null} and $Rag1/2^{null}\gamma c^{null}$ mice and the strains derived from them. In addition, the humanized mouse models used in studies of various human diseases will be summarized.

IMMUNODEFICIENT MICE

Since the discovery of nude and SCID mice,[5,6] humanized mice have been generated by using various immunodeficient mice. SCID mice that received human T and B cells by transplantation of fetal liver and thymus, which were termed *SCID-hu* mice by McCune *et al.*,[26,27] provided an attractive humanized model for research in various fields; however, engraftment rates were not high. In 1998, Goldman *et al.*[13] reported the enhanced engraftment of human cells in $Rag2^{null}$ mice possessing the IL-2Rγ^{null} gene. In the 2000s, a series of immunodeficient mice was developed by combining the IL-2Rγ^{null} gene with conventional SCID and $Rag1/2^{null}$ mice. These strains showed extremely high engraftment rates and differentiation of human cells, resulting in remarkable advances in the development of human disease models. These stains include the NOG (NOD/Shi-*Prkdc*^{scid} *Il2r*γ^{tm1Sug}/Jic) mice reported in 2002;[11] RG (BALB/c-$Rag2^{null}$Il2rγ^{null} (BRG) and C57BL/6-$Rag2^{null}$Il2rγ^{null} (B6RG)) mice reported in 1997, 1998 and 2004;[13,14,28] and NSG (NOD/LtSz-*Prkdc*^{scid} *Il2r*γ^{tm1Wjl}/J) mice reported in 2005.[12] Recently, immunodeficient BALB/c-$Rag1^{null}$Il2rγ^{null},[16] NOD-$Rag1^{null}$Il2rγ^{null},[15] and NOD/SCID-JaK3^{null} mice have been established as alternatives to NOG/NSG mice. Data accumulated to date suggest that NOG/NSG mice are the best recipients for humanized tissue and human cell engraftment occurs in the following order: NSG=NOG>NRG>BRG>NOD/SCID>B6RG.[15,16] The disadvantages of SCID and NOD/SCID mice include the frequent occurrence of thymic lymphoma and the leakiness, in which T and B cells develop in aged mice.[29,30] However, NOG mice show no leakiness or spontaneous thymic lymphoma.[31,32] This may be attributed to inactivation of IL-2Rγ, which is shared by important cytokines, such as IL-2, IL-4, IL-7, IL-15 and IL-21, each of which is important for T- and B-cell growth.[33] These results indicate that NOG/NSG mice are better recipients of human cells and tissues.

The most attractive feature of these humanized mice is the development of multilineage hematopoietic cells by transplantation of human HSCs. In particular, T-cell subpopulations, including CD4 and CD8 single positive cells, which could not be differentiated in NOD/SCID mice, successfully developed in these mice.[14,18,21] These results suggest the usefulness of humanized mice for investigating human immune responses. Indeed, the utility of these humanized mice is well accepted by researchers worldwide. However, these humanized mice are insufficient, since human cells are not fully functional. For example, no or rare antigen-specific IgG production occurs after multiple injections of antigens.[25]

To overcome this issue, various improved strains based on these immunodeficient mice have been developed or are being developed by several groups, including our group.[34,35] In Figure 1, the history of the development of immunodeficient humanized mice and their respective improvements are summarized. These mice have been established in NOG/NSG or BRG backgrounds. Background strain selection is crucial for the improvement of immunodeficient mice. In 1996, we reported human granulocyte–macrophage colony-stimulating factor (hGM-CSF) and interleukin-3 (IL-3) cosecreting transgenic (Tg) B6-SCID mice.[36] These strains were able to maintain human tumor cell lines possessing hGM-CSF and human IL-3 (hIL-3) receptors on the surface;[37] human cells, however, could not engraft in these mice. We recently established hGM-CSF/IL-3 Tg NOG mice by the conversion of strain B6 to NOG by backcross mating. High human cell engraftment rates were observed in hGM-CSF/IL-3 Tg NOG mice. We also compared engraftment of HSCs in NOG, BRG and B6RG mice. Higher engraftment rates were obtained in NOG and BRG, but not B6RG mice. In particular, we were surprised to detect only a few human cells in B6RG mice (unpubl. data). Similar results were reported by Traggiai *et al.*,[14] indicating that immunodeficient mice in a B6 background are not sufficient for generating humanized mice. Recent reports on signal regulatory protein (Sirpα) suggested that NOD mice are superior to other strains, because Sirpα in NOD strains is more similar to that in humans, compared with Sirpα in other mice strains.[38,39] Therefore, BRG transgenic mice with human Sirpα have been established to enhance human cell engraftment efficacy.[20]

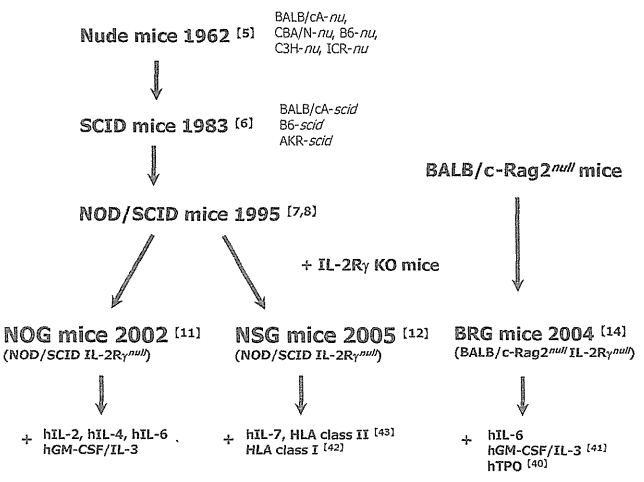

Figure 1 The history of the development on immunodeficient mice for humanized mice model. In retrospect, nude mice or SCID mice were the first immunodeficient strains. Subsequently, their congenic strains were generated to improve engraftment capacities. NOD/SCID mice established in 1995 have been a milestone in this field, because of the severer phenotype than nude and SCID mice. In early 2000s, NOG, NSG and BRG mice were established by introducing the IL-2Rγ^{null} allele into NOD/SCID or BALB/c $RAG2^{null}$ mice. Due to the complete loss of murine immune systems, human hematopoiesis has been enormously enhanced in these mice. Currently, these strains were further improved by introducing human genes for various cytokines or HLA class I and II, so as to recapitulate a human *bona fide* hematopoiesis and immune system. The superscripts represent the respective references. BRG, BALB/c-$Rag2^{null}$Il2rγ^{null}; HLA, histocompatibility leukocyte antigen; NOD, nonobese diabetic; NSG, NOD/LtSz-*Prkdc*^{scid} *Il2r*γ^{tm1Wjl}/J; SCID, severe combined immunodeficiency.

Improved strains were generated by injecting human DNA into pronuclear stage embryos, injecting genetically modified embryonic stem cells into blastocysts (knock-in (KI)), or introducing human genes by backcross mating with established transgenic mice. Specifically, human cell differentiation from HSCs in improved mice produced using the KI strategy has been analyzed by Flavell's group at the Yale University.[20] They reported elevated HSC and myeloid cell numbers in thrombopoietin (TPO) KI mice and increased alveolar Mϕ in hGM-CSF/IL-3 KI mice.[40,41] We also developed transgenic NOG mice that secreted human IL-2 or IL-4 by injecting DNA into NOG embryos. The suppression of graft-versus-host disease (GVHD) and dominant conversion to Th2 cells in hIL-4 Tβ NOG mice and remarkable differentiation of human NK cells in hIL-2 Tβ NOG mice, respectively, were observed (unpubl. data). Shultz's group generated human leukocyte antigen (HLA) class I transgenic NSG mice by backcross mating the respective transgenic mice into NSG mice. The successful generation of antigen-specific cytotoxic T cells[42] was observed. Antigen-specific IgG was produced in HLA class II transgenic NSG mice.[43]

Real humanized mice are expected to be generated in the near future by improving immunodeficient mice.

HEMATOLYMPHOID HUMANIZED MICE

The reconstitution of the human hematopoietic system is one of the most advanced areas in humanized mouse research. The use of NOG/NSG or BRG mice has greatly improved human hematopoiesis, as shown by the development of multiple human cell lineages, including B and T lymphocytes, NK cells, myeloid DC, plasmacytoid DC, Mϕ and erythroblasts. Here, we discuss the current status and perspectives in this field.

Lymphoid cells

Two major subsets of lymphoid cells, i.e., B and T cells, were developed in NOG mice by simply transferring human HSCs after irradiation.

B cells. Human B cells are detected in the PB 1 month after HSC transplantation and gradually increase in number over the following 3 months. In the BM, B-cell differentiation in humanized mice seems to consistently resemble that in humans, since several distinct precursor populations exist:[25] $CD19^-CD38^+CD10^+CD34^+$ early-B cells, $CD19^+IgM^-CD20^-CD34^+$ pro-B cells, $CD19^+IgM^-CD20^-CD34^-$ pre-B cells and $CD19^+IgM^+IgD^-$ immature B cells. The pro-B and pre-B populations were also characterized by the expression of intracellular V_{preB} and Cμ chains. In the spleen, one of the remarkable B-cell phenotypes in humanized mice is high CD5 expression, which is markedly different from genuine human B cells.[23] The significance of this upregulated CD5 expression remains controversial, i.e., whether these are human B-1 cells or transitional 1 B cells.[23,25]

Immunization of humanized mice with various exogenous substances induces antigen-specific IgM responses, suggesting that the B-cell repertoire is diverse and can cover a myriad of antigens.[21,23] Since antigen-specific IgG responses in conventional humanized mice are very weak,[14,21,23] it has been speculated that these B cells have some intrinsic defects in the class switch machineries. Several *in vitro* experiments, however, demonstrated that these B cells do produce IgG in response to stimulation through their antigen receptors and CD40 in the presence of IL-21.[25] In addition, recent reports have shown that new mouse strains that express HLA-DR mounted an antigen-specific IgG response upon immunization.[43] Collectively, B cells in humanized mice maintain the ability to mediate humoral immune reactions.

T cells. Human T cells can develop in humanized NOG/NSG or BRG mice in the thymus and accumulate in the spleen. This is one of the most important points of distinction from NOD/SCID mice, which only partially support the differentiation of human T cells. Typically, 3–5 months is necessary for T cells to colonize the spleen.[44] In the thymus, human thymocytes show typical surface phenotypes,[44] i.e., $CD4^-CD8^-$, $CD4^+CD8^+$, $CD4^-CD8^+$ and $CD4^+CD8^-$ stages, suggesting that they follow the normal differentiation pathway. The thymus is indispensable for T-cell development, and selection is largely mediated by mouse major histocompatibility complex (MHC) molecules, given that Foxn1-deficient NOG mice (NOG *nu/nu*) cannot support T-cell development, and $CD4^+$ and $CD8^+$ T cells do not fully develop in NOG I-$A\beta^{null}$ or NOG $\beta2m^{null}$ backgrounds,[25] respectively.

Although development seems to be relatively normal, the functionality of T cells in humanized mice remains controversial. For example, in studies using Epstein–Barr virus (EBV), humanized mice showed antiviral T-cell responses in which interferon-γ producing $CD8^+$ T cells were differentiated and protected mice from lymphoma development,[14,45] thus supporting the normal functions of human $CD8^+$ T cells. However, *in vitro* experiments have suggested that human T cells have a limited ability to respond to antigenic stimulation.[25] Although the mechanisms underlying abnormal T-cell functions remain unclear, mismatches between mouse MHC and the HLA of donor human cells may be involved. Indeed, HLA-A- or HLA-DR-expressing NSG mice showed normal cytotoxic reactions (cytotoxic T-lymphocyte responses) to viral infection or IgG responses against exogenous antigens, respectively.[43,46,47]

NK cells. Human NK cells also develop from the early stage (4 weeks) of HSC transfer. However, the number of NK cells is not very high (a low percentage of human $CD45^+$ cells), indicating the necessity for growth and differentiation factors in immunodeficient mice.[48] Huntington *et al.*[49] reported that the hIL-15/hIL-15Rα complex induces extensive proliferation and differentiation of $CD16^+KIR^+$ NK cells. Chen *et al.*[50] also reported that administering IL-15 and the Flt-3/Flk-2 ligand by plasmid DNA injection into HSC-transferred mice leads to an increased number of NK cells. In IL-2 Tg NOG mice (Katano *et al.*, manuscr. in prep.), human NK cells predominantly develop prior to B and T cells after HSC transfer, and consist of the largest population in human $CD45^+$ cells. However, their function has not been well characterized.

As an alternative method for studying human NK cell functions, *ex vivo* isolated human NK cells from peripheral blood mononuclear cells (PBMCs) have been transplanted into NOG mice. Although the inoculated NK cells were not maintained in these mice for a long time, the cells exerted effective antibody-dependent cellular cytotoxicity and suppressed the growth of a Burkitt's lymphoma cell line (Daudi), following concomitant administration of an anti-CD20 antibody (rituximab).[51]

Myeloid cells

In conventional humanized mice, although human myeloid cells were shown to be differentiated, the efficiency was poor. Recently, however, the development of various lineages of myeloid cells has been improved by introducing human cytokines.

Monocytes. Human monocytes/Mϕ can be detected in the blood, lymphoid organs (spleen and BM) and some tissue organs (lung and liver) in conventional humanized mice. The frequency of human $CD14^+$ cells among the total human $CD45^+$ cell population is usually not more than 1%–2% in the spleen, while the frequency can reach 8% or 5% in

the lungs or liver, respectively. The delivery of plasmid DNA encoding several human cytokine genes,[50] i.e., IL-15 with Flt-3 ligand (Flt3L) or macrophage CSF, by hydrodynamic injection robustly induces the development of human monocytes/Mϕ in various organs. In addition, in a novel mouse strain in which the TPO gene was replaced with the human homolog, the development of total human myeloid lineage cells was significantly improved.[40] Accordingly, the frequency of monocytes was increased in the blood, but not in the BM. In our studies, the transgenic expression of hIL-3 and GM-CSF genes in NOG (hGM-CSF/IL-3 Tβ NOG) mice also improved the development of whole human myeloid cells, including $CD14^+$ monocytes (Ito *et al.*, manuscr. submitt.).

DCs. In conventional humanized mice, several reports have demonstrated the presence of both myeloid DCs ($CD11c^+HLA\text{-}DR^+CD40^+CD86^+$) and plasmacytoid DCs ($CD123^+HLA\text{-}DR^+BDCA2^+$) in the BM, spleen and liver.[14,50] These $CD11c^+$ or $CD123^+$ DCs were functional, as demonstrated by their ability to induce activation of allogeneic human T cells or to produce interferon-α after stimulation.[14] The frequency of these cells, however, is generally low in the spleen (typically less than 1% in our studies). Chen *et al.*[50] demonstrated that the administration of plasmid DNA encoding human IL-4/GM-CSF/Flt3L or IL-5/Flt3L markedly increased the DC yield.[50] Enhancements in DC development were also observed in our hGM-CSF/IL-3 Tβ NOG mice, in terms of both number and frequency, in various lymphoid organs (Ito *et al.*, manuscr. submitt.).

Granulocytes. Although granulocytes comprise a large fraction of human leukocytes, their frequency in humanized mice is very low (less than 2%–3% of human leukocytes in PB and BM in our studies). To improve differentiation of this population, several groups have attempted to produce novel humanized mouse strains by providing human cytokines. Billerbeck *et al.*[52] created a transgenic NSG strain that expressed the human stem cell factor, GM-CSF and IL-3 genes, and demonstrated a slight increased development of human $CD15^+$ granulocytes in the BM. In TPO KI mice, as mentioned above, a large number of human $CD66b^+$ granulocytes were produced in the BM.[40] Moreover, this strain enabled the development of mature human neutrophils with lobulated nuclei, which has not been achieved before. Additionally, in our hGM-CSF/IL-3 Tβ NOG mice, we confirmed significant increases in $CD66b^+$ granulocyte numbers in the BM and PB. Furthermore, the presence of human basophils and eosinophils in the PB was detected by May–Giemsa staining (Ito *et al.*, manuscr. submitt.). This is the first report to demonstrate the development of these cell populations in humanized mice. Collectively, the development of human granulocytes in humanized mice has been greatly improved by the addition of human cytokines.

Mast cells. Mast cells play an important role in allergic responses by releasing intracellular granules containing histamine or various leukotrienes. Crosslinking of their surface Fc-epsilon receptor (FcεR) by IgE triggers a series of reactions.[53,54] Although there is little evidence suggesting the development of human mast cells, Kambe *et al.*[55] demonstrated the presence of human mast cells in the skin, spleen and BM of humanized NOG mice. These cells were positive for c-kit and CD203c, but expression of FcεR was not determined. Recently, we detected FcεR positive mast cells in the BM, spleen and several non-lymphoid tissues of hGM-CSF/IL-3 Tβ NOG mice (Ito *et al.*, manuscr. submitt.). These data suggest that IL-3 and/or GM-CSF are important for inducing the differentiation of human mast cells.

HUMANIZED MODELS

Cancer

Due to their supply by the Central Institute for Experimental Animals, NOG mice have been predominantly used in this field. The characteristics of NOG mice include rapid growth of tumors and well-maintained characteristics after multiple passages. In a study by Machida *et al.*,[56] 100 HeLa S3 cells could be successfully engrafted in NOG mice; in contrast, 10^5 and 10^6 cells were required for engraftment in NOD/SCID and C.B-17-SCID mice, respectively. However, primary human tumors do not always engraft in NOG mice, even though these animals show higher engraftment than conventional immunodeficient mice. Some tumors, such as prostate carcinoma, which are difficult to engraft in SCID and nude mice, are also difficult to engraft in NOG mice. The growth of some tumor cell lines appears to be less than in conventional immunodeficient mice. The reason for this is unclear, but it may be explained by the differential adaptation of cell lines to conventional immunodeficient mice. *IL-2Rγ* gene inactivation may influence the growth of some tumors in NOG mice. Another characteristic of NOG mice is a high occurrence of metastasis. Genes responsible for metastasis have been investigated through the use of this characteristic.[57] The high homing capacity of human cells also appears to be maintained in NOG mice. When U266 myeloma cells were intravenously injected into NOG mice, they grew only in the BM, resulting in paralysis.[58]

Various cancer models have been established using these advantages.[51,59] On the other hand, a model that can be used to investigate immune responses to tumors has only recently been developed. Mismatching of HLA between tumor cells and hematopoietic cells from HSCs of different donors may cause severe GVHD or a lack of response. To induce an effective immune response against tumors in mice, HLA matching is required. Recently, Shultz *et al.*[42] reported that antigen-specific cytotoxic T lymphocytes were successfully induced in a newly established HLA class I (A-2) transgenic NSG mouse model by transfer of HLA-matched HSC. The development of these mice may lead to new immunotherapy models for cancer. The injection of human PBMCs (hPBMCs) into immunodeficient mice is known to cause severe GVHD; this provides a good model of GVHD.[60] We recently found that NOG-I-$A\beta^{null}\beta2m^{null}$ mice showed mild GVHD, although high engraftment rates were observed as compared with non-transgenic NOG mice after transfer of hPBMCs (unpubl. data). Cotransplantation of a patient's tumor and hPBMCs into such immunodeficient mice may facilitate analysis of the immunological responses to the tumor.

Infectious diseases

Human lymphocytes, including T and B cells, predominantly develop in humanized mice transferred with HSCs. Therefore, appropriate models are provided for viruses that specifically infect lymphocytes and express their pathology, such as HIV-1, HTLV-1 and EBV. HIV-1 infection models have been widely used for the analysis of disease mechanisms and the development of anti-HIV-1 drugs,[61] as HIV-1 infects human T cells in *SCID-hu* mice.[26,62,63] This research is further accelerated through the use of HSC-transplanted immunodeficient mice, in which multilineage hematopoietic cells can be differentiated.[64–67] In this field, a unique model for HIV-1[68–70] reported by Garcia's group at the University of North Carolina and termed bone marrow–liver–thymus (BLT) mice, has attracted attention. As the name suggests, this model is generated by transplantation of fetal bone marrow, liver and thymus into a subcutaneous region of the kidney. The most attractive feature of BLT mice is reconstitution of human

mucosal immunity; this has not yet been obtained in human immune system mice transferred with HSCs. The human mucosal lymphoid apparatus, including Peyer's patches and gut-associated lymphoid tissue, has been successfully reconstituted in BLT mice, resulting in the development of mucosal immunity. They reported that the *IL-2Rγ* gene was indispensable for development of the mucosal lymphoid system, indicating that mucosal immunity cannot develop in NOG/NSG and BRG mice that contain a mutant *Il2rγ* gene (reported at the Third International Workshop of Humanized Mice (IWHM 2011) held in Pittsburgh in October 2011).

This mouse appears to provide a better HIV-1 model as compared with conventional humanized mice transferred with HSCs. However, this model cannot be investigated from the aspect of humoral immunity involving B cells, and cannot be used in some countries such as Japan because of ethical issues. Additional genetic modifications of current immunodeficient mice may be necessary to overcome this disadvantage.

EBV usually presents in healthy subjects as a latent infection; however, it expresses a variety of pathological features in the healthy, termed EBV-associated infectious mononucleosis, hemophagocytic lymphohistiocytosis, lymphoproliferative disease, Burkitt's lymphoma and Hodgkin's disease in those immunosuppressed, due to HIV-1 infection or BM transplantation.[71] Since the report of EBV-associated lymphoproliferative disease by Traggiai *et al.*[14] using humanized BRG mice, various humanized mouse models of these clinical pathologies have been reported.[72–74]

Humanized models of tuberculosis, salmonellosis, yellow fever and Dengue fever have been investigated.[75–77]

Animal models appropriate for developing a malaria vaccine are eagerly desired, as malaria is one of the most common infectious diseases worldwide.[78] An interesting human malaria model uses immunodeficient mice with transplanted human liver. By injecting human hepatocytes into liver-damaged immunodeficient mice,[79–82] human hepatocytes replace the mouse hepatocytes. In these hu-liver mice, intrahepatic multiplication of *Plasmodium falciparum* has been observed.[83] However, human erythrocytes from human blood must be successively injected into the mice intraperitoneally, because human erythrocytes cannot develop from HSCs.[84] To establish the complete malaria life cycle in mouse models, it is necessary to develop mice in which human erythrocytes persist and flow in mouse peripheral blood. Hu-liver mice provide a good infection model for viruses specific to hepatocytes, including hepatitis C and B viruses.[85–87]

These models provide invaluable tools for analyzing the mechanisms of human infection and for developing chemotherapeutic agents such as antibodies.

GVHD

GVHD is a severe complication with a high mortality rate that often develops in patients who receive allogeneic BM transplantation for the treatment of acute/chronic leukemia, aplastic anemia or congenital immunodeficiency. Approximately 20 years ago, Mosier *et al.*[63] first demonstrated that the induction of xenogenic GVHD was possible in immunodeficient mice (C.B-17-SCID) by transplanting hPBMCs. In this model, the transplanted human T cells may be activated and attack the recipient mouse tissue, thus resulting in the development of allogeneic GVHD-like symptoms.

Although C.B-17-SCID or NOD/SCID mice have been useful in GVHD research, there are several problems. For example, human cell engraftment is relatively low, due to the mouse endogenous innate immune system. It also requires sublethal dose total body irradiation, which results in large variances in disease onset. Furthermore, a relatively large number of hPBMCs have to be administered intraperitoneally, but not intravenously, to induce the disease.[88] This does not reflect BM transplantation, where cells are infused intravenously. van Rijn *et al.*[89] used H-2^{d}-$RAG2^{null}$ $IL2r\gamma^{null}$ mice in which xeno-GVHD was induced by intravenous injection of hPBMCs; however, this model still depends on the infusion of large numbers of hPBMCs (3×10^{7} cells/head) and total body irradiation. Our xeno-GVHD NOG mouse model has shown significant improvements over other models, such as the rapid onset of disease and uniform death of recipients. In addition, a smaller number of donor cells (2.5×10^{6}) is sufficient with intravenous injection, and total body irradiation is not always necessary.[60] These results were confirmed by other studies using NSG mice.[90]

Collectively, NOG or NSG mice are the most suitable platforms for basic and preclinical GVHD research at this time.

Humanized liver models

Humanized liver models, in which the mouse liver is replaced with a human liver, are useful for evaluating drug metabolism in the human liver, as there are numerous differences in liver enzymes between humans and mice. In the first human liver model developed by Mercer *et al.*,[81] SCID/*bg* mice carrying a urokinase-type plasminogen activator transgene (Alb-uPA) entered a profound hypofibrinogenemic state, which caused hepatocyte death. They transplanted human hepatocytes into the inferior splenic pole and demonstrated that human hepatocytes could be engrafted over 50% in the liver of these mice. To improve xenoengraftment of human hepatocytes, NOG-uPA[82] and FRG (fumarylacetoacetate $hydrolase^{null}$/$RAG2^{null}$/IL-$2R\gamma^{null}$)[79] mice, in which liver damage is induced by adenovirus-mediated uPA expression, were developed and showed markedly high rates of replacement by human hepatocytes (over 80%). Nevertheless, several problems limit their utility, such as poor breeding efficiency in the mouse colony, development of renal disease, and a very narrow time window for transplantation. Recently, Hasegawa *et al.*[80] established a novel NOG substrain that expresses the herpes simplex virus type 1 thymidine kinase (TK) transgene under the control of a mouse albumin promoter. Administration of ganciclovir, which is non-toxic to human and mouse tissues, ablated TK-expressing liver parenchymal cells. Herpes simplex virus type 1 TK NOG mice allowed high engraftment of human hepatocytes (over 80%) and did not develop systemic morbidity (liver disease, renal disease and bleeding diathesis) as seen in other uPA-dependent models. Stable, long-term humanization of TK NOG mice will facilitate studies of drug metabolism, toxicology and the virology of hepatitis viruses.

FUTURE PERSPECTIVES

Over the last 10 years, remarkable progress has been achieved in humanized mouse models using NOD/SCID/γc^{null}, $Rag1/2^{null}\gamma c^{null}$ mice, especially for hematology and immunology. Various humanized mouse models have been established that enable direct research of human diseases, which was previously impossible in immunocompetent animals. These models will also contribute to the analysis of mechanisms underlying human immune disorders and the development of vaccines against infectious diseases through the use of humanized mice that contain a wide variety of functional human hematopoietic cells.

However, several issues remain to be overcome, such as the rare differentiation of certain cell lineages from HSCs, immature differentiation and insufficient intercellular relationships. To overcome these problems, the inclusion of other immunodeficient mouse genes

or human genes responsible for cell differentiation and interaction has been investigated. These attempts may result in more appropriate immunodeficient humanized mice.

Recently, progress in the field of regenerative medicine has drawn our attention, following the establishment of human embryonic stem and inducible pluripotent stem cells. In the future, artificial human organs or HSCs developed from embryonic stem or inducible pluripotent stem cells may be available. Although these techniques have not yet impacted the field of humanized mice, new models will likely result from transplantation of artificial human organs and HSCs.

ACKNOWLEDGEMENTS

This research was supported by a Grant-in-Aid for Scientific Research from the Ministry of Education, Culture, Sports, Science, and Technology (MEXT), by a grant (22A-9) from the National Center for Child Health and Development, and by a grant from Research on Emerging and Re-emerging Infectious Diseases from Ministry of Health, Labour and Welfare, Japan.

1 Shultz LD, Ishikawa F, Greiner DL. Humanized mice in translational biomedical research. *Nat Rev Immunol* 2007; **7**: 118–130.
2 Ito M, Kobayashi K, Nakahata T. NOD/Shi-*scid IL2r*γ^{null} (NOG) mice more appropriate for humanized mouse models. *Curr Top Microbiol Immunol* 2008; **324**: 53–76.
3 Legrand N, Weijer K, Spits H. Experimental models to study development and function of the human immune system *in vivo*. *J Immunol* 2006; **176**: 2053–2058.
4 Zhang B, Duan Z, Zhao Y. Mouse models with human immunity and their application in biomedical research. *J Cell Mol Med* 2009; **13**: 1043–1058.
5 Issacson J, Cattanach B. Report. *Mouse News Lett* 1962; **27**: 31.
6 Bosma GC, Custer RP, Bosma MJ. A severe combined immunodeficiency mutation in the mouse. *Nature* 1983; **301**: 527–530.
7 Shultz LD, Schweitzer PA, Christianson SW, Gott B, Schweitzer IB, Tennent B *et al*. Multiple defects in innate and adaptive immunologic function in NOD/LtSz-*scid* mice. *J Immunol* 1995; **154**: 180–191.
8 Koyanagi Y, Tanaka Y, Tanaka R, Misawa N, Kawano Y, Tanaka T *et al*. High levels of viremia in *hu*-PBL-NOD-*scid* mice with HIV-1 infection. *Leukemia* 11997; Suppl 3, 109–112.
9 Christianson SW, Greiner DL, Hesselton RA, Leif JH, Wagar EJ, Schweitzer IB *et al*. Enhanced human CD4$^+$ T cell engraftment in β2-microglobulin-deficient NOD-*scid* mice. *J Immunol* 1997; **158**: 3578–3586.
10 Shultz LD, Banuelos S, Lyons B, Samuels R, Burzenski L, Gott B *et al*. NOD/LtSz-Rag1^{null}Pfp^{null} mice: a new model system with increased levels of human peripheral leukocyte and hematopoietic stem-cell engraftment. *Transplantation* 2003; **76**: 1036–1042.
11 Ito M, Hiramatsu H, Kobayashi K, Suzue K, Kawahata M, Hioki K *et al*. NOD/SCID/γ_c^{null} mouse: an excellent recipient mouse model for engraftment of human cells. *Blood* 2002; **100**: 3175–3182.
12 Shultz LD, Lyons BL, Burzenski LM, Gott B, Chen X, Chaleff S *et al*. Human lymphoid and myeloid cell development in NOD/LtSz-*scid IL2R*γ^{null} mice engrafted with mobilized human hemopoietic stem cells. *J Immunol* 2005; **174**: 6477–6489.
13 Goldman JP, Blundell MP, Lopes L, Kinnon C, Di Santo JP, Thrasher AJ. Enhanced human cell engraftment in mice deficient in RAG2 and the common cytokine receptor gamma chain. *Br J Haematol* 1998; **103**: 335–342.
14 Traggiai E, Chicha L, Mazzucchelli L, Bronz L, Piffaretti JC, Lanzavecchia A *et al*. Development of a human adaptive immune system in cord blood cell-transplanted mice. *Science* 2004; **304**: 104–107.
15 Pearson T, Shultz LD, Miller D, King M, Laning J, Fodor W *et al*. Non-obese diabetic-recombination activating gene-1 (NOD-Rag1^{null}) interleukin (IL)-2 receptor common gamma chain (IL2rγ^{null}) null mice: a radioresistant model for human lympho-haematopoietic engraftment. *Clin Exp Immunol* 2008; **154**: 270–284.
16 Brehm MA, Cuthbert A, Yang C, Miller DM, DiIorio P, Laning J *et al*. Parameters for establishing humanized mouse models to study human immunity: analysis of human hematopoietic stem cell engraftment in three immunodeficient strains of mice bearing the *IL2r*γ^{null} mutation. *Clin Immunol* 2010; **135**: 84–98.
17 Yahata T, Ando K, Nakamura Y, Ueyama Y, Shimamura K, Tamaoki N *et al*. Functional human T lymphocyte development from cord blood CD34$^+$ cells in nonobese diabetic/Shi-*scid*, IL-2 receptor γnull mice. *J Immunol* 2002; **169**: 204–209.
18 Hiramatsu H, Nishikomori R, Heike T, Ito M, Kobayashi K, Katamura K *et al*. Complete reconstitution of human lymphocytes from cord blood CD34$^+$ cells using the NOD/SCID/γc^{null} mice model. *Blood* 2003; **102**: 873–880.
19 Ishikawa F, Shimazu H, Shultz LD, Fukata M, Nakamura R, Lyons B *et al*. Purified human hematopoietic stem cells contribute to the generation of cardiomyocytes through cell fusion. *FASEB J* 2006; **20**: 950–952.
20 Willinger T, Rongvaux A, Strowig T, Manz MG, Flavell RA. Improving human hemato-lymphoid-system mice by cytokine knock-in gene replacement. *Trends Immunol* 2011; **32**: 321–327.
21 Ishikawa F, Yasukawa M, Lyons B, Yoshida S, Miyamoto T, Yoshimoto G *et al*. Development of functional human blood and immune systems in NOD/SCID/IL2 receptor γ chain^{null} mice. *Blood* 2005; **106**: 1565–1573.
22 Lepus CM, Gibson TF, Gerber SA, Kawikova I, Szczepanik M, Hossain J *et al*. Comparison of human fetal liver, umbilical cord blood, and adult blood hematopoietic stem cell engraftment in NOD-*scid*/$\gamma c^{-/-}$, Balb/c-Rag1$^{-/-}\gamma c^{-/-}$, and C.B-17-*scid/bg* immunodeficient mice. *Hum Immunol* 2009; **70**: 790–802.
23 Matsumura T, Kametani Y, Ando K, Hirano Y, Katano I, Ito R *et al*. Functional CD5$^+$ B cells develop predominantly in the spleen of NOD/SCID/γc^{null} (NOG) mice transplanted either with human umbilical cord blood, bone marrow, or mobilized peripheral blood CD34$^+$ cells. *Exp Hematol* 2003; **31**: 789–797.
24 Hayakawa J, Hsieh MM, Uchida N, Phang O, Tisdale JF. Busulfan produces efficient human cell engraftment in NOD/LtSz-*Scid IL2R*γ^{null} mice. *Stem Cells* 2009; **27**: 175–182.
25 Watanabe Y, Takahashi T, Okajima A, Shiokawa M, Ishii N, Katano I *et al*. The analysis of the functions of human B and T cells in humanized NOD/shi-*scid*/γc^{null} (NOG) mice (hu-HSC NOG mice). *Int Immunol* 2009; **21**: 843–858.
26 McCune J, Kaneshima H, Krowka J, Namikawa R, Outzen H, Peault B *et al*. The *SCID-hu* mouse: a small animal model for HIV infection and pathogenesis. *Annu Rev Immunol* 1991; **9**: 399–429.
27 McCune JM, Namikawa R, Kaneshima H, Shultz LD, Lieberman M, Weissman IL. The *SCID-hu* mouse: murine model for the analysis of human hematolymphoid differentiation and function. *Science* 1988; **241**: 1632–1639.
28 Kirberg J, Berns A, von Boehmer H. Peripheral T cell survival requires continual ligation of the T cell receptor to major histocompatibility complex-encoded molecules. *J Exp Med* 1997; **186**: 1269–1275.
29 Custer RP, Bosma GC, Bosma MJ. Severe combined immunodeficiency (SCID) in the mouse. Pathology, reconstitution, neoplasms. *Am J Pathol* 1985; **120**: 464–477.
30 Bosma MJ. B and T cell leakiness in the *scid* mouse mutant. *Immunodefic Rev* 1992; **3**: 261–276.
31 Kato C, Fujii E, Chen YJ, Endaya BB, Matsubara K, Suzuki M *et al*. Spontaneous thymic lymphomas in the non-obese diabetic/Shi-*scid*, *IL-2R*γ^{null} mouse. *Lab Anim* 2009; **43**: 402–404.
32 Katano I, Ito R, Eto T, Aiso S, Ito M. Immunodeficient NOD-*scid IL-2R*γ^{null} mice do not display T and B cell leakiness. *Exp Anim* 2011; **60**: 181–186.
33 Sugamura K, Asao H, Kondo M, Tanaka N, Ishii N, Ohbo K *et al*. The interleukin-2 receptor gamma chain: its role in the multiple cytokine receptor complexes and T cell development in XSCID. *Annu Rev Immunol* 1996; **14**: 179–205.
34 Okada S, Harada H, Ito T, Saito T, Suzu S. Early development of human hematopoietic and acquired immune systems in new born NOD/Scid/Jak3^{null} mice intrahepatic engrafted with cord blood-derived CD34$^+$ cells. *Int J Hematol* 2008; **88**: 476–482.
35 Sato Y, Takata H, Kobayashi N, Nagata S, Nakagata N, Ueno T *et al*. Failure of effector function of human CD8$^+$ T cells in NOD/SCID/JAK3/ immunodeficient mice transplanted with human CD34$^+$ hematopoietic stem cells. *PLoS One* 2010; **5**: e13109.
36 Miyakawa Y, Fukuchi Y, Ito M, Kobayashi K, Kuramochi T, Ikeda Y *et al*. Establishment of human granulocyte–macrophage colony stimulating factor produing transgenic SCID mice. *Br J Haematol* 1996; **95**: 437–442.
37 Fukuchi Y, Miyakawa Y, Kobayashi K, Kuramochi T, Shimamura K, Tamaoki N *et al*. Cytokine dependent growth of human TF-1 leukemic cell line in human GM-CSF and IL-3 producing transgenic SCID mice. *Leuk Res* 1998; **22**: 837–843.
38 Takenaka K, Prasolava TK, Wang JC, Mortin-Toth SM, Khalouei S, Gan OI *et al*. Polymorphism in Sirpa modulates engraftment of human hematopoietic stem cells. *Nat Immunol* 2007; **8**: 1313–1323.
39 Takizawa H, Manz MG. Macrophage tolerance: CD47-SIRP-α-mediated signals matter. *Nat Immunol* 2007; **8**: 1287–1289.
40 Rongvaux A, Willinger T, Takizawa H, Rathinam C, Auerbach W, Murphy AJ *et al*. Human thrombopoietin knockin mice efficiently support human hematopoiesis *in vivo*. *Proc Natl Acad Sci USA* 2011; **108**: 2378–2383.
41 Willinger T, Rongvaux A, Takizawa H, Yancopoulos GD, Valenzuela DM, Murphy AJ *et al*. Human IL-3/GM-CSF knock-in mice support human alveolar macrophage development and human immune responses in the lung. *Proc Natl Acad Sci USA* 2011; **108**: 2390–2395.
42 Shultz LD, Saito Y, Najima Y, Tanaka S, Ochi T, Tomizawa M *et al*. Generation of functional human T-cell subsets with HLA-restricted immune responses in HLA class I expressing NOD/SCID/IL2rγ^{null} humanized mice. *Proc Natl Acad Sci USA* 2010; **107**: 13022–13027.
43 Danner R, Chaudhari SN, Rosenberger J, Surls J, Richie TL, Brumeanu TD *et al*. Expression of HLA class II molecules in humanized NOD.Rag1KO.IL2RgcKO mice is critical for development and function of human T and B cells. *PLoS One* 2011; **6**: e19826.
44 Hiramatsu H, Nishikomori R, Heike T, Ito M, Kobayashi K, Katamura K *et al*. Complete reconstitution of human lymphocytes from cord blood CD34$^+$ cells using the NOD/SCID/γc^{null} mice model. *Blood* 2003; **102**: 873–880.
45 Yajima M, Imadome K, Nakagawa A, Watanabe S, Terashima K, Nakamura H *et al*. T cell-mediated control of Epstein–Barr virus infection in humanized mice. *J Infect Dis* 2009; **200**: 1611–1615.
46 Shultz LD, Saito Y, Najima Y, Tanaka S, Ochi T, Tomizawa M *et al*. Generation of functional human T-cell subsets with HLA-restricted immune responses in HLA class I expressing NOD/SCID/IL2rγ^{null} humanized mice. *Proc Natl Acad Sci USA* 2010; **107**: 13022–13027.
47 Strowig T, Gurer C, Ploss A, Liu YF, Arrey F, Sashihara J *et al*. Priming of protective T cell responses against virus-induced tumors in mice with human immune system components. *J Exp Med* 2009; **206**: 1423–1434.

48 Suwanai H, Wilcox MA, Mathis D, Benoist C. A defective *Il15* allele underlies the deficiency in natural killer cell activity in nonobese diabetic mice. *Proc Natl Acad Sci USA* 01;**107**: 9305–9310.
49 Huntington ND, Legrand N, Alves NL, Jaron B, Weijer K, Plet A *et al.* IL-15 trans-presentation promotes human NK cell development and differentiation *in vivo*. *J Exp Med* 2009; **206**: 25–34.
50 Chen Q, Khoury M, Chen J. Expression of human cytokines dramatically improves reconstitution of specific human-blood lineage cells in humanized mice. *Proc Natl Acad Sci USA* 2009; **106**: 21783–21788.
51 Shiokawa M, Takahashi T, Murakami A, Kita S, Ito M, Sugamura K *et al.* *In vivo* assay of human NK-dependent ADCC using NOD/SCID/γc^{null} (NOG) mice. *Biochem Biophys Res Commun* 2010; **399**: 733–737.
52 Billerbeck E, Barry WT, Mu K, Dorner M, Rice CM, Ploss A. Development of human $CD4^+FoxP3^+$ regulatory T cells in human stem cell factor-, granulocytenmacrophage colony-stimulating factor-, and interleukin-3-expressing NOD-SCID IL2Rγ^{null} humanized mice. *Blood* 2011; **117**: 3076–3086.
53 Williams CM, Galli SJ. The diverse potential effector and immunoregulatory roles of mast cells in allergic disease. *J Allergy Clin Immunol* 2000; **105**: 847–859.
54 Galli SJ, Wershil BK. The two faces of the mast cell. *Nature* 1996; **381**: 21–22.
55 Kambe N, Hiramatsu H, Shimonaka M, Fujino H, Nishikomori R, Heike T *et al.* Development of both human connective tissue-type and mucosal-type mast cells in mice from hematopoietic stem cells with identical distribution pattern to human body. *Blood* 2004; **103**: 860–867.
56 Machida K, Suemizu H, Kawai K, Ishikawa T, Sawada R, Ohnishi Y *et al.* Higher susceptibility of NOG mice to xenotransplanted tumors. *J Toxicol Sci* 2009; **34**: 123–127.
57 Suemizu H, Monnai M, Ohnishi Y, Ito M, Tamaoki N, Nakamura M. Identification of a key molecular regulator of liver metastasis in human pancreatic carcinoma using a novel quantitative model of metastasis in NOD/SCID/γc^{null} (NOG) mice. *Int J Oncol* 2007; **31**: 741–751.
58 Miyakawa Y, Ohnishi Y, Tomisawa M, Monnai M, Kohmura K, Ueyama Y *et al.* Establishment of a new model of human multiple myeloma using NOD/SCID/γc^{null} (NOG) mice. *Biochem Biophys Res Commun* 2004; **313**: 258–262.
59 Ninomiya M, Kiyoi H, Ito M, Hirose Y, Naoe T. Retinoic acid syndrome in NOD/*scid* mice induced by injecting an acute promyelocytic leukemia cell line. *Leukemia* 2004; **18**: 442–448.
60 Ito R, Katano I, Kawai K, Hirata H, Ogura T, Kamisako T *et al.* Highly sensitive model for xenogenic GVHD using severe immunodeficient NOG mice. *Transplantation* 2009; **87**: 1654–1658.
61 Zhang L, Meissner E, Chen J, Su L. Current humanized mouse models for studying human immunology and HIV-1 immuno-pathogenesis. *Sci China Life Sci* 2010; **53**: 195–203.
62 Namikawa R, Kaneshima H, Lieberman M, Weissman IL, McCune JM. Infection of the *SCID-hu* mouse by HIV-1. *Science* 1988; **242**: 1684–1686.
63 Mosier DE, Gulizia RJ, Baird SM, Wilson DB. Transfer of a functional human immune system to mice with severe combined immunodeficiency. *Nature* 1988; **335**: 256–259.
64 Koyanagi Y, Tanaka Y, Ito M, Yamamoto N. Humanized mice for human retrovirus infection. *Curr Top Microbiol Immunol* 2008; **324**: 133–148.
65 Sato K, Nie C, Misawa N, Tanaka Y, Ito M, Koyanagi Y. Dynamics of memory and naive $CD8^+$ T lymphocytes in humanized NOD/SCID/IL-2Rγ^{null} mice infected with CCR5-tropic HIV-1. *Vaccine* 82010; Suppl 2, B32–37.
66 Watanabe S, Ohta S, Yajima M, Terashima K, Ito M, Mugishima H *et al.* Humanized NOD/SCID/IL2Rγ^{null} mice transplanted with hematopoietic stem cells under nonmyeloablative conditions show prolonged life spans and allow detailed analysis of human immunodeficiency virus type 1 pathogenesis. *J Virol* 2007; **81**: 13259–13264.
67 Watanabe S, Terashima K, Ohta S, Horibata S, Yajima M, Shiozawa Y *et al.* Hematopoietic stem cell-engrafted NOD/SCID/IL2Rγ^{null} mice develop human lymphoid systems and induce long-lasting HIV-1 infection with specific humoral immune responses. *Blood* 2007; **109**: 212–218.
68 Denton PW, Estes JD, Sun Z, Othieno FA, Wei BL, Wege AK *et al.* Antiretroviral pre-exposure prophylaxis prevents vaginal transmission of HIV-1 in humanized BLT mice. *PLoS Med* 2008; **5**: e16.
69 Olesen R, Wahl A, Denton PW, Garcia JV. Immune reconstitution of the female reproductive tract of humanized BLT mice and their susceptibility to human immunodeficiency virus infection. *J Reprod Immunol* 2011; **88**: 195–203.
70 Choudhary S, Archin N, Cheema M, Dahl N, Garcia JV, Margolis D. Latent HIV-1 infection of resting $CD4^+$ T cells in the humanized $Rag2^{-/-}\gamma c^{-/-}$ mouse. *J Virol* 2012; **86**: 114–120.
71 Rickinson AB, Kieff E. Epstein–Barr virus. In:Knipe DM, Howley PM (eds.) Fields virology. Philadelphia: Lippincott Williams & Wilkins, 2011: 2575–2628.
72 Yajima M, Imadome K, Nakagawa A, Watanabe S, Terashima K, Nakamura H *et al.* A new humanized mouse model of Epstein–Barr virus infection that reproduces persistent infection, lymphoproliferative disorder, and cell-mediated and humoral immune responses. *J Infect Dis* 2008; **198**: 673–682.
73 Sato K, Misawa N, Nie C, Satou Y, Iwakiri D, Matsuoka M *et al.* A novel animal model of Epstein–Barr virus-associated hemophagocytic lymphohistiocytosis in humanized mice. *Blood* 2011; **117**: 5663–5673.
74 Imadome K, Yajima M, Arai A, Nakazawa A, Kawano F, Ichikawa S *et al.* Novel mouse xenograft models reveal a critical role of $CD4^+$ T cells in the proliferation of EBV-infected T and NK cells. *PLoS Pathog* 2011; **7**: e1002326.
75 Song J, Willinger T, Rongvaux A, Eynon EE, Stevens S, Manz MG *et al.* A mouse model for the human pathogen *Salmonella typhi*. *Cell Host Microbe* 2010; **8**: 369–376.
76 Libby SJ, Brehm MA, Greiner DL, Shultz LD, McClelland M, Smith KD *et al.* Humanized nonobese diabetic-*scid IL2r*γ^{null} mice are susceptible to lethal *Salmonella typhi* infection. *Proc Natl Acad Sci USA* 2010; **107**: 15589–15594.
77 Firoz Mian M, Pek EA, Chenoweth MJ, Ashkar AA. Humanized mice are susceptible to *Salmonella typhi* infection. *Cell Mol Immunol* 2011; **8**: 83–87.
78 Sauerwein RW, Roestenberg M, Moorthy VS. Experimental human challenge infections can accelerate clinical malaria vaccine development. *Nat Rev Immunol* 2011; **11**: 57–64.
79 Azuma H, Paulk N, Ranade A, Dorrell C, Al-Dhalimy M, Ellis E *et al.* Robust expansion of human hepatocytes in $Fah^{-/-}/Rag2^{-/-}/Il2rg^{-/-}$ mice. *Nat Biotechnol* 2007; **25**: 903–910.
80 Hasegawa M, Kawai K, Mitsui T, Taniguchi K, Monnai M, Wakui M *et al.* The reconstituted 'humanized liver' in TK-NOG mice is mature and functional. *Biochem Biophys Res Commun* 2011; **405**: 405–410.
81 Mercer DF, Schiller DE, Elliott JF, Douglas DN, Hao C, Rinfret A *et al.* Hepatitis C virus replication in mice with chimeric human livers. *Nat Med* 2001; **7**: 927–933.
82 Suemizu H, Hasegawa M, Kawai K, Taniguchi K, Monnai M, Wakui M *et al.* Establishment of a humanized model of liver using NOD/Shi-*scid* IL2Rg^{null} mice. *Biochem Biophys Res Commun* 2008; **377**: 248–252.
83 Mikolajczak SA, Sacci JB Jr, de la Vega P, Camargo N, VanBuskirk K, Krzych U *et al.* Disruption of the *Plasmodium falciparum* liver-stage antigen-1 locus causes a differentiation defect in late liver-stage parasites. *Cell Microbiol* 2011; **13**: 1250–1260.
84 Jimenez-Diaz MB, Mulet T, Viera S, Gomez V, Garuti H, Ibanez J *et al.* Improved murine model of malaria using *Plasmodium falciparum* competent strains and non-myelodepleted NOD-*scid IL2R*γ^{null} mice engrafted with human erythrocytes. *Antimicrob Agents Chemother* 2009; **53**: 4533–4536.
85 Bissig KD, Wieland SF, Tran P, Isogawa M, Le TT, Chisari FV *et al.* Human liver chimeric mice provide a model for hepatitis B and C virus infection and treatment. *J Clin Invest* 2010; **120**: 924–930.
86 Haridass D, Yuan Q, Becker PD, Cantz T, Iken M, Rothe M *et al.* Repopulation efficiencies of adult hepatocytes, fetal liver progenitor cells, and embryonic stem cell-derived hepatic cells in albumin-promoter-enhancer urokinase-type plasminogen activator mice. *Am J Pathol* 2009; **175**: 1483–1492.
87 Washburn ML, Bility MT, Zhang L, Kovalev GI, Buntzman A, Frelinger JA *et al.* A humanized mouse model to study hepatitis C virus infection, immune response, and liver disease. *Gastroenterology* 2011; **140**: 1334–1344.
88 Martino G, Anastasi J, Feng J, Mc Shan C, DeGroot L, Quintans J *et al.* The fate of human peripheral blood lymphocytes after transplantation into SCID mice. *Eur J Immunol* 1993; **23**: 1023–1028.
89 van Rijn RS, Simonetti ER, Hagenbeek A, Hogenes MC, de Weger RA, Canninga-van Dijk MR *et al.* A new xenograft model for graft-versus-host disease by intravenous transfer of human peripheral blood mononuclear cells in $RAG2^{-/-}$ $\gamma c^{-/-}$ double-mutant mice. *Blood* 2003; **102**: 2522–2531.
90 King MA, Covassin L, Brehm MA, Racki W, Pearson T, Leif J *et al.* Human peripheral blood leucocyte non-obese diabetic-severe combined immunodeficiency interleukin-2 receptor gamma chain gene mouse model of xenogeneic graft-versus-host-like disease and the role of host major histocompatibility complex. *Clin Exp Immunol* 2009; **157**: 104–118.